Chem Soc Rev

REVIEW ARTICLE

View Article Online
View Journal | View Issue

Check for updates

Cite this: *Chem. Soc. Rev.*, 2025, **54**, 8325

Bioinspired helical systems with defined chirality assembled from discrete peptide and glycan amphiphiles

Vânia I. B. Castro, [ab] Rui L. Reis, [ab] Ricardo A. Pires *[ab] and Iva Pashkuleva *[ab]

Molecular helices are ubiquitous in biological systems and play key roles in life functions such as recognition, coding and transferring information, replication, catalytic activity, among others. They can have different handedness and dimensions from molecular to macroscale but the exact mechanisms for their formation are still elusive. *In vivo*, they are formed from homochiral building blocks (L-amino acids and D-carbohydrates) by complex, orchestrated supramolecular aggregation processes. Thus, self-assembly of synthetic chiral analogues of these blocks has been explored to understand the underlying principles of supramolecular chirality, their importance in (supra)molecular biorecognition in the physiological environment, as well as to develop novel functional biomaterials. In this review, we discuss the role of different factors in the formation of supramolecular helices and the definition of handedness in model systems composed by peptides and carbohydrates: the effect(s) of the chirality and sequence in the building blocks, (non)chiral additives, assembly conditions, *i.e.* co-solvent, pH, temperature are showcased. The possibility to tune these factors towards assembly of helices with defined chirality is also discussed and supported by recent examples from the literature. Finally, we explore the importance of these assemblies in different bioapplications.

Received 12th May 2025

DOI: 10.1039/d5cs00158g

rsc.li/chem-soc-rev

Open Access Article. Published on 13 August 2025. Downloaded on 1/7/2026 10:35:48 PM.
This article is licensed under a Creative Commons Attribution 3.0 Unported Licence.

[a] *3B's Research Group, I3Bs – Research Institute on Biomaterials, Biodegradables and Biomimetics, University of Minho, Headquarters of the European Institute of Excellence on Tissue Engineering and Regenerative Medicine, 4608-017 Barco, Portugal. E-mail: rpires@i3bs.uminho.pt, pashkuleva@i3bs.uminho.pt*
[b] *ICVS/3B's PT Government Associated Laboratory, Braga/Guimaraes, Portugal*

1. Introduction

The term chirality has a Greek origin (χειρ, kheir) and means "hand" – a body part commonly used to demonstrate non-superimposable symmetry that is an essential characteristic of

Vânia I. B. Castro

Vânia I. B. Castro has a BSc in chemistry and MSc in medicinal chemistry. In 2025, she finished her PhD studies in the field of supramolecular chemistry at the 3B's Research Group, University of Minho. She is interested in the development of supramolecular biomaterials for regenerative medicine. During the last years, she has been working on the design and synthesis of short peptides and amphiphiles that can be used as low molecular weight gelators. Particular emphasis has been given to the development of helical systems for biomedical applications. Currently, Vânia is a postdoctoral fellow and keeps her interest in supramolecular systems.

Rui L. Reis

Rui L. Reis is a full professor of tissue engineering, regenerative medicine and stem cells at the University of Minho, Portugal where he is also leading 3Bs Research Group and the Research Institute on Biomaterials, Biodegradables and Biomimetics. He has been working in the field of biomaterials for more than 30 years. Hallmark of his research is the use of natural resources and biomolecules for the development of functional devices and materials by non-conventional processing methodologies. The developed biomaterials are used in different approaches for tissue regeneration and in the establishment of 3D disease models.

Open Access Article. Published on 13 August 2025. Downloaded on 1/7/2026 10:35:48 PM.
This article is licensed under a Creative Commons Attribution 3.0 Unported Licence.

the chiral objects. In chemistry, the term was introduced by Lord Kelvin in 1894 but the molecular chirality was demonstrated earlier, in 1848, by Louis Pasteur who separated two crystal forms of tartaric acid salts that when dissolved rotated the plane of light at the same angle, but in opposite directions.[1] In 1874, Le Bel and van't Hoff independently presented theories that can explain the molecular basis of the optical properties observed by Pasteur.[2] These theories are the basis of the stereochemistry and postulate that chirality can be observed only for molecules with an asymmetric centre, usually an sp^3 carbon, whose substituents are all different (Fig. 1a).[2,3]

Chiral pairs have identical atomic composition but different spatial arrangement that results in different interaction with polarised light, thus, they are defined as optical isomers or enantiomers. There are several nomenclatures used to distinguish chiral molecules. IUPAC recommends the application of the Cahn–Ingold–Prelog rules that determine the configuration of the asymmetric centre as R (rectus/right) or S (sinister/left).

Conventional D/L nomenclature is commonly used for amino acids and carbohydrates and is based on the rotation of polarised light clockwise (dextrorotatory, D) and counter clockwise (laevorotatory, L) by these molecules. There is no relation between these two nomenclatures: while most natural amino acids have L-configuration they can be either R, for example cysteine, or S for any other natural L-amino acid and this is because Cahn–Ingold–Prelog rules give priority to –SH groups (priority order: –SH, –OH, $–NH_2$, –COOH, –CHO, $–CH_2OH$, $–C_6H_5$, –D, –H).

The stereochemistry, and in particular chirality, is an important mean for coding and transferring information in living systems, where chiral molecules exist mostly as single enantiomers.[5] The domination of L-amino acids and D-carbohydrates in biosynthesis of informational polymers (proteins, DNA, and RNA) is one of the fundamental questions related with the origin of life that is yet to be answered. Empirical evidences show that proteins built from L-amino acids usually fold into right-handed α-helices and β-strands,

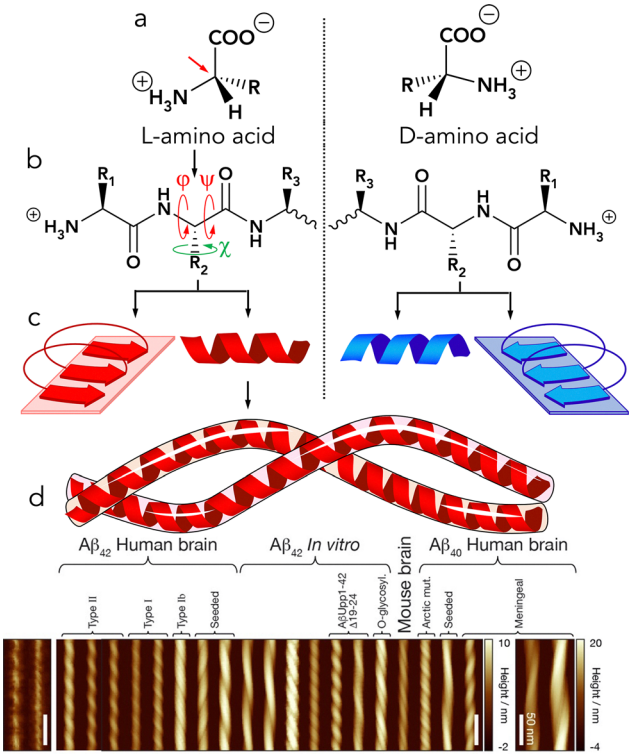

Fig. 1 Chirality of the amino acids and its transfer at different levels. (a) The amino acids have one chiral centre (red arrow) that makes possible two isomers: L- and D-amino acids. Biological systems use mostly L-amino acids to build their proteome. (b) In the polypeptide backbone the torsion angles φ and ψ (designated in red) describe the rotation of the protein backbone and define the secondary structure of proteins. Side chains can also have different torsion angles χ (in green). (c) The canonical proteins comprising L-amino acids usually fold into right-handed α-helices and twisted β-strands (red), while synthetic polypeptides comprising D-amino acids form left-handed helices and β-strands (blue). (d) The helices can further interact by supramolecular interactions often resulting in a polymorphism as shown for Aβ42 fibrils (Reproduced with permissions from ref. 4).

Ricardo A. Pires

Ricardo A. Pires is a principal investigator at 3Bs Research Group, University of Minho. He holds PhD in materials engineering. During the last 15 years, he has been involved in the biomedical field where he investigates the supramolecular interactions of peptides and carbohydrates. His research is relevant to the area of bionanotechnology as it can be applied for the development of functional biomimics of different pathological environemnts (e.g. cancer) as well as to the areas of biochemistry and neurosciences for providing mechanistic understanding of the pathological proteins aggregation and the related neurodegenerative disorders.

Iva Pashkuleva

Iva Pashkuleva has a PhD in organic chemistry and currently, she is a principal investigator at 3Bs Research Group. She is interested in biomimetic systems that copycat the biochemical and morphological features of the extracellular matrix. Supramolecular interactions of glycans and glycosaminoglycans have a privileged place in her research: specifically designed copolymers and amphiphiles that assemble at physiological conditions or in response to physiological stimuli are used by her either to elucidate the mechanisms of cellular communication or as components of different therapies that affect this communication.

This journal is © The Royal Society of Chemistry 2025

Open Access Article. Published on 13 August 2025. Downloaded on 1/7/2026 10:35:48 PM.
This article is licensed under a Creative Commons Attribution 3.0 Unported Licence.

while synthetic peptides comprising non-canonical D-amino acids form left-handed helices (Fig. 1b).[6–8] However, there are many exceptions because these processes are quite complex in life systems, where the environment is abundant in chiral molecules and biosynthesis can favour out of equilibrium pathways and products, *e.g.* protein misfolding. Additionally, further supramolecular packing and stacking of the α-helices and β-strands in coils and sheets often involve polymorphism (Fig. 1c) due to the low energy barriers between different forms. As a result, not all chiral building blocks assemble into chiral structures and the same chiral components can generate structures with different morphologies and handedness.

The complexity is even higher for carbohydrates because each optical isomer (D- or L-) has 4 asymmetric centres in their open-chain (aldose or ketose) forms (Fig. 2a, red arrows), thus increasing the number of stereoisomers according to Le Bel–van't Hoff rule. Monosaccharides also exist in cyclic form, so-called hemiacetal forms, in which an additional asymmetric carbon is formed (Fig. 2b, red arrow) increasing the number of possible stereoisomers (Fig. 2c). Additionally, the flexibility of non-planar hemiacetal forms allows for several puckered conformations (Fig. 2d). Of note, all these stereoisomers have different supramolecular interactome. For example, different carbohydrate puckers influence the interactions of the nucleotides in the nucleic acids and impact the structure and the function of DNA and RNA. Theoretically, such stereochemical wealth allows the development of specific chiral signatures that diversify the biological functions, however, the experimental development and control of such specific structures are challenging.[9–11]

Like proteins, polysaccharides can adopt secondary structures – ribbon-like (*e.g.* cellulose, chitin) and helical conformations (*e.g.* amylose, agarose, carrageenans, β-1,3 glucans, β-1,3 xylans, glycosaminoglycans) with different flexibility and ability to organise in higher hierarchical structures.[12,13] When compared to proteins, the diversity of polysaccharides' secondary structures is higher due to monosaccharides puckering (Fig. 2d) and flexibility of the glycosidic bond.[9,14]

For example, polysaccharide helices have a pitch between 7 and 47 Å (*vs.* 5.4 Å for protein's α-helices) and can be either right- (β-1,3 glucans, β-1,3 xylans, carrageenans) or left-handed (amylose, agarose, glycosaminoglycans).[13] The high flexibility and heavy involvement of H-bonding in stabilisation of the polysaccharides secondary (or higher order) structures make the studies in aqueous solutions very challenging.[10]

Thus, the development of synthetic helical structures with controlled handedness is of upmost interest for better understanding the chirality in biological environments and discovery of biofunctional artificial systems. Various helical nanostructures, such as twisted nanofibres, helical ribbons, rolled-up nanotubes, and superhelices (Fig. 3) have been developed using different approaches and building blocks.[15–17] Herein, we focus on supramolecular approaches involving peptides and carbohydrates in aqueous environment, given their importance in biological systems. In these approaches chiral transfer and/or amplification is achieved *via* non-covalent interactions and thus, it is dynamic and dependent on the environment – just like in the life systems. We discuss different building blocks and experimental conditions that favour the assembly of helical

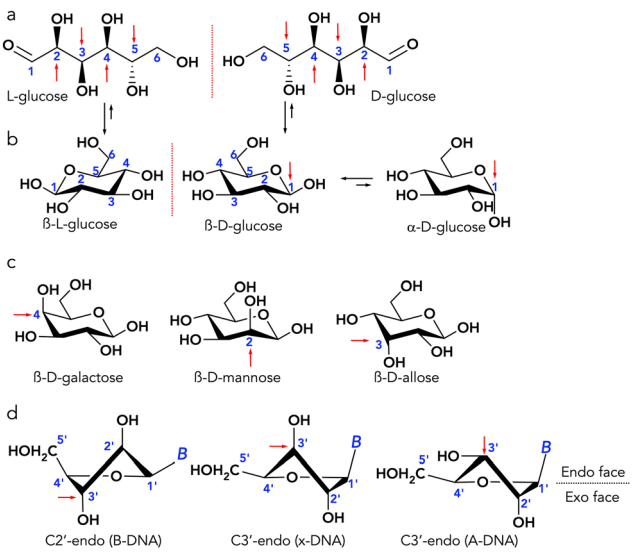

Fig. 2 Stereochemical wealth of carbohydrates. Biological systems use D-monosaccharides to make their glycome: (a) the linear monosaccharides have four asymmetric centres (red arrows). (b) Cyclic forms of the monosaccharides exist in equilibrium with their open-chain forms and have one additional asymmetric carbon – so-called anomeric carbon (red arrows). (c) Each monosaccharide has several epimers that differ by the stereochemistry of one asymmetric centre (red arrows). (d) Monosaccharides have different puckered forms, *e.g.* the showed puckers of 2-deoxyribose (the position of the base in the nucleoside is denoted with B) influence the helical conformation in DNA: A-DNA and B-DNA are right-handed helices, x-DNA has no specific conformation and z-DNA has left-handed helical conformation, in which C2′-*endo* and C3′-*endo* puckered forms are alternated.

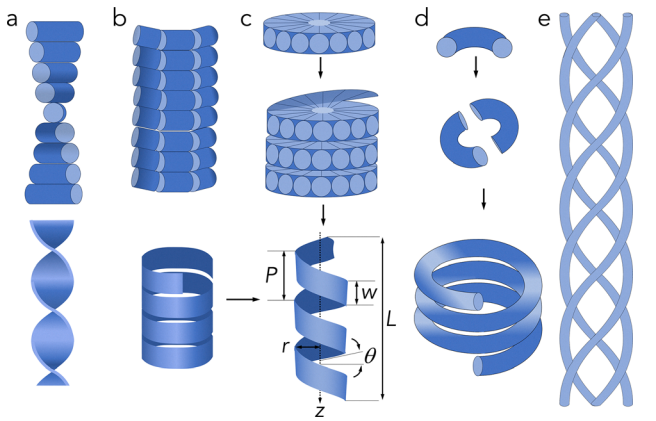

Fig. 3 Examples of supramolecular helical structures discussed in this review (the assembling molecules are presented as cylinders): (a) helical tape in which the molecules are in chain-like order; (b) helical ribbons, in which the molecules are in a sheet-like arrangement; (c) helices obtained by association of micellar discs (the parameters used for description of the helical structures are presented: *z* - axis of curvature, *L* - length, *P* - pitch, *w* - width, *r* - radius of curvature, *θ* - gradient angle); (d) helices obtained by polymerisation of helical monomers; (e) coiled-coil superhelices.

Open Access Article. Published on 13 August 2025. Downloaded on 1/7/2026 10:35:48 PM.
This article is licensed under a Creative Commons Attribution 3.0 Unported Licence.

structures. The bioapplications of the obtained assemblies are also discussed.

2. Supramolecular polymerisation, chirality, and helicity

Supramolecular chemistry and self-assembly processes are ubiquitously used by living systems to develop functional structures by autonomous organisation of molecular components. In particular, unidirectional (1D) self-assembly results in the formation of supramolecular polymers – analogues of conventional covalent polymers, in which the self-assembling molecules (monomers) are organised in long chains but held together by supramolecular interactions.[18] Examples are the helical actin filaments and microtubules that are essential components of cytoskeleton with crucial roles in cell shape, locomotion and intracellular transport.

As any spontaneous process, the supramolecular polymerisation tends to reach minimum Gibbs free energy (ΔG, eqn (1)) that defines the thermodynamic stability of the system. The polymerisation is driven by the attractive forces between the monomers that decrease the enthalpy contribution (ΔH) to ΔG. Such disorder to order transition results in apparent entropy (ΔS) decrease. To maintain negative ΔG, the entropic loss must be compensated, and this balance is achieved by the release of water molecules solvating the monomers, thus, increasing the entropy of the water. Therefore, the hydration dynamics and local water organisation are important elements in the process.[9,19]

$$\Delta G = \Delta H - T\Delta S \quad (1)$$

In aqueous media, most supramolecular polymers are formed by either isodesmic or cooperative mechanism.[20] The isodesmic mechanism refers to uniform association of monomers to a growing supramolecular chain. Such step-growth mechanism results in assembly of flexible supramolecular chains and is described by a single association constant that does not depend on the chain length. Less flexible supramolecular polymers are obtained by the alternative cooperative mechanism that has two phases – an initial nucleation step followed by fibre growth, each of which is described by different association constants. Further details about these mechanisms can be found in several excellent reviews.[18,20,21]

When the molecules that participate in the self-assembly process are arranged non symmetrically, a supramolecular chirality emerges.[15] Supramolecular helices are examples of chiral structures as they have non-superimposable symmetry (Fig. 4). While the characteristics of the covalent helices depend mainly on the relative order of the monomers in the backbone (*e.g.* the amino acids in protein helices) and usually the smallest possible loop is adopted and fixed, supramolecular helices are looser and dynamic due to the involvement of different repulsive and attractive physical forces between the building blocks.

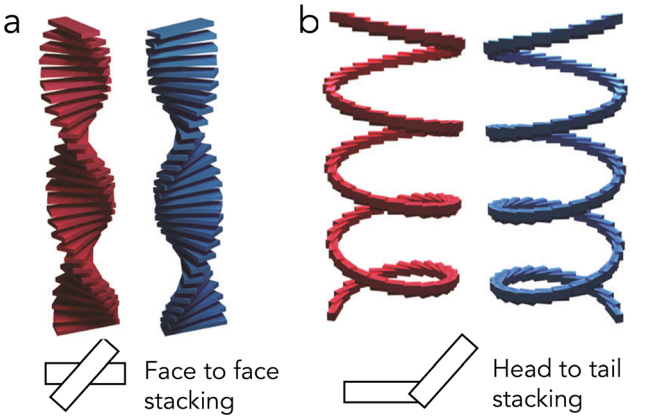

Fig. 4 Schematic presentation of helical structures assembled *via* (a) asymmetric H-type and (b) asymmetric J-type organisations. Each block segment in the structures represents a self-assembling molecule (monomer). Right-handed (P) assemblies are presented in blue and left-handed (M) helices are shown in red. Reproduced with permission from ref. 22 Copyright 2021, Royal Society of Chemistry.

There are different types of supramolecular organisation and interactions that can lead to formation of coiled or twisted structures but in all of them chiral molecules pack at a slight angle with respect to their neighbours (Fig. 4). In H-type supramolecular polymers, for example, the monomers are aligned parallel and stack in a face-to-face mode (Fig. 4a). In J-type helices, the monomers arrange in a head-to-tail fashion, with the transition dipoles aligned to favour coupling in a linear-like fashion (Fig. 4b).

It is expected that in aqueous solutions amphiphiles should organise in a manner to shield the hydrophobic portion from water and expose their hydrophilic groups. Flat (bi)layers and spherical vesicles are the anticipated assemblies but experimental data evidenced that many chiral amphiphiles form helical tubes and twisted ribbons (Fig. 3). While these supramolecular structures are morphologically defined as 1D helices, they are usually formed by rolling 2D (bi)layered membranes, *i.e.* they are formed by different mechanisms. Several models have been proposed to explain the formation of curved structures but the ones that fit better with the experimental results are the models based on chiral elastic properties.[23] The fundament of these models is that the stacking at small angle favours long-range twisting at the direction of the molecules organisation. A major shortcoming of most of the proposed models is the assumption of continuous system instead of an ensemble of discreate chiral units with specific shape. Boden *et al.* outstripped partially this drawback and proposed a model in which a chiral β-sheet forming peptide is represented as chiral rod-like monomer (Fig. 5a).[24] According to this model, the attraction between the monomers results in assembly of tapes – a step that requires minimal energy for the conformational adjustment of the peptides (ε_{trans}, Fig. 5a). The tapes are helical due to the chirality of the monomers and have different faces (represented in white and grey in Fig. 5b) that depend on the peptide composition and can be designed to have different affinity to water. The distinct hydrophobicity of both sides of

 This journal is © The Royal Society of Chemistry 2025

Open Access Article. Published on 13 August 2025. Downloaded on 1/7/2026 10:35:48 PM. This article is licensed under a Creative Commons Attribution 3.0 Unported Licence.

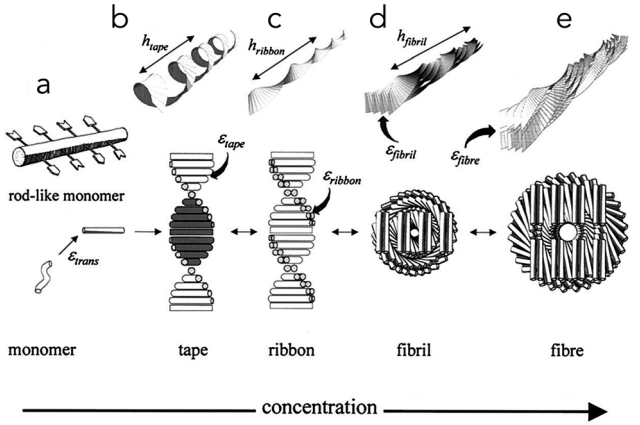

Fig. 5 Model of hierarchical self-assembly of (a) chiral peptides represented as rod monomers. (b)–(e) Different helical assemblies (upper row) and the respective global equilibrium conformation (down row) for the supramolecular helices formed in solutions of chiral molecules. (b) At low concentration, the monomers interact *via* complementary donor and acceptor groups (shown by arrows in (a)) and align to form tapes. At higher concentration, the tapes further stack into (c) ribbons, (d) fibrils, and (e) fibres. Adapted with permission from ref. 24 Copyright (2001) National Academy of Sciences.

the tapes can give rise to further stacking towards ribbons and then between ribbons to form assemblies with higher hierarchical organisation (Fig. 5b–e). Such hierarchical stacking requires adjustment of the helical twist to fit packing constrains. The energy needed for the adjustments is termed elastic energy and must be compensated by the attraction energies coming from the stacking between types, ribbons, and fibrils. This balance determines the morphology of the final assembly.

While neglected in most models, the amphiphile structure and shape are important as they determine the stacking angle. On the other hand, the bending of the assembled structure depends also on the long length scale degree of freedom. It can result in twisted (Fig. 3a) or helical ribbons (Fig. 3b and c). These structures are different – while twisted ribbons have a Gaussian-like curvatures, helical ribbons have a cylindrical curvature (Fig. 3c). The difference is not straightforward and experimental data showed that twisted ribbons can be transformed into helical ribbons: Pashuck and Stupp showed that peptide amphiphiles initially (seconds) form short twisted ribbons that with the time (minutes) elongate and ultimately (weeks) transform into helical ribbons.[25] This transition suggests that the twisted ribbons might be kinetic products (see Section 4.2 for definition) resulting from inhomogeneous twist, in which the periphery of the β-sheet is less bended, and reorganisation towards optimal packing lead to the thermodynamically stable helical ribbons.

Fuhrhop *et al.* put forward another mechanism for the formation of helical ribbons from *N*-alkylaldonamides.[26] They proposed that helical ribbons can be formed upon a reorganisation of micelles above their critical micelle concertation (CMC), when occurs a conversion to micellar discs followed by stacking of the discs (Fig. 3c). In this model, the bended geometry of the molecule is essential for the helical formation (further discussed in Section 4.1).

For helical structures, the terms P (plus) and M (minus) are used to describe the handedness: the right-handed helices (helix twists in a clockwise direction as it moves away from the observer) are designated as P-helices, while the left-handed helices (helix that twists in a counterclockwise direction) are assigned as M-helices. Besides the handedness, supramolecular helices are described by other parameters (Fig. 3c) such as their length, diameter/radius of curvature, and chiral pitches that can vary from few nanometres to millimetres.

3. Induction of chirality

There is a consensus that the handedness of supramolecular helices depends on the chirality of the building blocks but the mechanisms of the asymmetry propagation through space and length scales are elusive. A theoretical concept called "parity violation energy difference" has been introduced to explain this process. The theory describes a small energy difference (in the order of 10^{-15} to 10^{-13} eV) between different enantiomers caused by weak nuclear forces.[27,28] While it can explain theoretically the emergence of homochirality and asymmetry propagation, it cannot be proven experimentally because of its extremely low magnitude that is overpowered by other interactions as thermal effects and quantum noise. Thus, self-assembly of specifically designed short peptide and carbohydrate amphiphiles have been instrumental in understanding the helical development and chirality propagation from one level to another.[6,11] As an example, self-replicating peptides have been used to demonstrate how structural information is propagated under prebiotic conditions, providing insight into molecular evolution and the possible pathways for the origin of life.[29–31] In these studies, complementary methods are used for characterisation of the assemblies: wide-angle X-ray scattering (WAXS) and spectroscopy techniques such as circular dichroism (CD), vibrational CD (VCD), and Raman optical activity (ROA) spectroscopy, give information about the molecular organisation and chirality, while microscopy techniques such as atomic force microscopy (AFM), high resolution scanning electron microscopy (SEM) and transmission electron microscopy (TEM) are used for visualisation of the assembled helical structures (*e.g.* nanoribbons, nanohelices) and elucidation of their handedness and hierarchical organisation at nano-/microscopic level.[22,32]

Supramolecular chirality can emerge from non-covalent interactions between chiral molecules, but also when achiral molecules assemble in the presence of chiral components.[33] The process in which a small chiral bias is significantly enhanced through covalent binding is called chiral amplification and was introduced in the 1980s by Green who studied a series of covalent polyisocyanates with stiff helical conformation.[34,35] The right- and left-handed helical conformations of these polyisocyanates are readily reversable due to the small energy barrier and thus, the polymerisation of achiral isocyanates in the presence of a small amount of a chiral component results in

Open Access Article. Published on 13 August 2025. Downloaded on 1/7/2026 10:35:48 PM.
This article is licensed under a Creative Commons Attribution 3.0 Unported Licence.

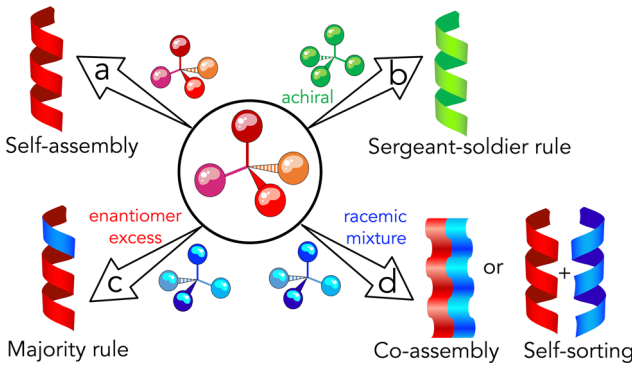

Fig. 6 Schematic presentation of common ways used to induce amplification of asymmetry in (a) helical supramolecular systems: (b) achiral molecules assemble in the presence of a chiral component; (c) enantiomers mixture with excess of one component; and (d) equimolar mixtures of enantiomers (racemates).

optically active copolymers.[35] This process has been compared to an army organisation, in which a few sergeants (chiral component) can control the movements of large number of cooperative soldiers (achiral monomers), and is commonly defined as sergeants-and-soldiers rule.[34] Green has also demonstrated that a small excess of one enantiomer in mixtures can lead to the formation of helices whose conformation is biased towards the component present in excess, *i.e.* helical sense is ruled by the majority and this bias is known as majority rule.[36] These rules are also applied to supramolecular polymers (Fig. 6a–c).[17,37–39] For example, addition of chiral peptide auxiliaries appended with naphthalenediimides to their achiral analogue in a typical sergeants-and-soldiers experiment leads to the assembly of helical structure with handedness corresponding to the added chiral component.[38]

The analogy between chirality induction in covalent and supramolecular systems is not absolute and some characteristics related with the dynamics of the supramolecular assembly must be considered. The chiral memory effect is a particular application of the sergeants-and-soldiers rule, in which a chiral agent is used to impart chirality in systems assembled from achiral building blocks or induce chirality bias in racemic mixtures and then is removed or replaced without affecting the induced chirality.[40,41] While this approach has been widely applied to covalent polymers, its implementation for supramolecular systems is embarrassed by the dynamic exchange of structural components – the introduction of a chiral agent can induce disassembly by disturbing the interactions that hold the structure together instead of inducing chiral amplification.[40] However, there are several examples in which the memory effect has been successfully demonstrated for supramolecular peptide-based systems.[38,40]

In the case of supramolecular systems, it is recommended the use of the term amplification of asymmetry instead of amplification of chirality.[17] This term describes the non-linear increase of the enantiomeric excess, optical activity, and net helicity in the assembled system.[17,42] The use of this terminology is particularly relevant in the case of supramolecular chiral structures assembled from synthetic peptides and glycans because these building blocks can be homo- (all D- or all L-) or heterochiral (comprising both D- and L-amino acids and monosaccharides, respectively).

The possibility for the amplification of the asymmetry in racemic mixtures, *i.e.* the self-assembly of equimolar mixtures of D- and L-enantiomers (Fig. 6d), has been studied thoroughly. In 1953, Pauling and Corey predicted that racemates of L- and D-peptides should pack into rippled β-sheet structure composed by alternating L- and D-sequences (Fig. 7a), *i.e.* they should co-assemble.[43] Since then, different mixtures of synthetic peptides and glycans have been studied.[6,11,44–46] Because helical structures are readily visualized by high resolution microscopies, they are very convenient for these studies. Nilsson *et al.* have shown that indeed racemate of homochiral L- and D-peptide FKFEFKFE co-assembled into rippled β-sheet structure.[45] The TEM analysis showed that enantiomer pure peptides formed helical ribbons with opposite helicity, while the racemate assembled into flat nanoribbon structures (Fig. 7b). Similar behaviour has been also reported for *N*-alkyl-glyconamides and aromatic disaccharides.[11,26,47]

Such preference towards co-assembly can be explained by several factors. From a statistical point of view, racemates have more packing options than single enantiomers and thus, the probability to form thermodynamically stable assemblies is higher. Kinetic factor can also contribute to this preference: in co-assembly both enantiomers can propagate the growth by binding on the nucleus (initial small cluster of assembling blocks), whereas in self-sorting an inhibition of the growth can occur if the "wrong" enantiomer binds to the cluster of the other stereoisomer.

Besides these factors, kinetically entrapped (for definition see Section 4.2) self-sorting and formation of mixture of helices

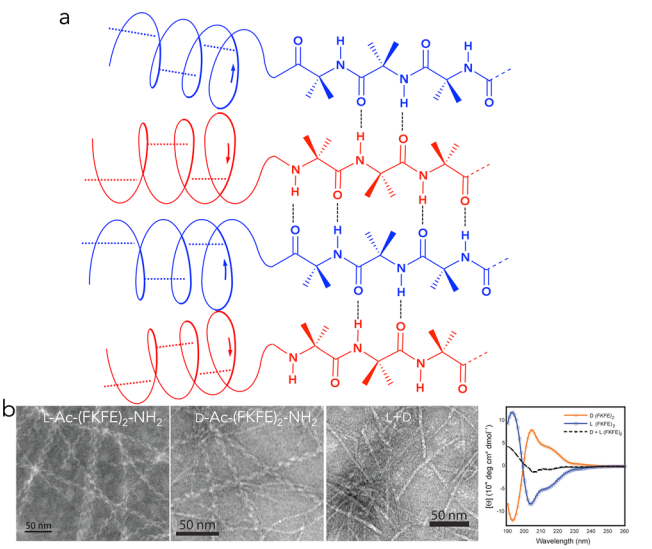

Fig. 7 Examples of different processes that can occur in racemates self-assembly. (a) Schematic presentation of the rippled β-sheet structure composed by alternating L- and D-sequences. Adapted with permission from ref. 44 Copyright 1987 by John Wiley and Sons. (b) Helical fibres of homochiral L- and D-peptide FKFEFKFE and the respective co-assembly obtained from their racemate (L + D). Reprinted with permission from ref. 45. Copyright 2012 American Chemical Society.

This journal is © The Royal Society of Chemistry 2025

Open Access Article. Published on 13 August 2025. Downloaded on 1/7/2026 10:35:48 PM. This article is licensed under a Creative Commons Attribution 3.0 Unported Licence.

with opposite handedness can take place.[48] Recent data from Stupp *et al.* suggests that self-sorting occurs due to the enthalpic penalty required to change the twist.[49] The complexity of the assembled helical structure can also contribute – often the formed self-sorting helixes are complex superstructures (*e.g.* coiled coils) as indicated by their size and their formation implies perturbing of the molecular packing. It is expected that a manipulation of the temperature would result in reorganisation of self-sorted helixes and formation of more stable co-assembled structure. Indeed, experimental data indicate that fast cooling of racemate solutions can promote self-sorting, while slow cooling enhances co-assembly.

4. Control of supramolecular helicity

The formation of supramolecular helices from discrete low molecular weight components is a complex process governed by the interplay of different factors, broadly divided into two categories – molecular and environmental factors. The thermodynamics of the system is related with the molecular design, while the kinetics relies on environmental factors. Understanding and controlling these factors is therefore essential for the design and synthesis of helical supramolecular assemblies with targeted properties.

4.1. Molecular factors

Rational design of the assembling blocks, *i.e.* low molecular weight peptide and carbohydrate amphiphiles, is a straightforward approach to control the helicity and handedness of the system by tuning the supramolecular interactome involved in the assembly.[9,11,50–53] Early studies have established the main rules for molecular design: the assembling blocks must be chiral, amphiphilic, and contain a rigid segment and amide bond(s).[54,55] Indeed, most of the reported supramolecular helices are assembled from peptide and carbohydrate amphiphiles that follow these rules although some exceptions exist.

The rigid segments determine the pseudocrystalline organisation of the helical assembly. The amide bonds are essential for the formation of directional intermolecular H-bonding and studies have shown that the replacement of amide with ester functionality compromise the formation of unidirectional assemblies. In aqueous environment, however, the directional H-bonding between short amphiphiles is weakened and must be strengthened by hydrophobic interactions, π-stacking, electrostatic interactions, and/or metal-ion coordination. Thus, in addition to H-bonds formed between intermolecular amides, an introduction of rigid alkyl portion or π-stacking motifs by functionalisation with aromatic groups such as fluorenylmethoxycarbonyl (Fmoc), naphthylmethyl (Nap) or adjustment of the content of aromatic amino acids in short peptides is a common strategy to enhance the assembly propensity and overall stability of supramolecular helices in aqueous environment as well as to control the handedness.[56–58]

The fine balance between hydrophobic and hydrophilic regions within the amphiphiles is critical because it tunes the solubility and the type of inter- and intramolecular interactions that will drive the assembly process and assure the stability of the helical structure. As an example, Welte and Pfannemuller have studied different *N*-alkyl-D-gluconamides, in which the length of the alkyl chain varies between C_6 and C_{10} and found that only *N*-octyl-D-gluconamide forms exclusively helical assemblies that are right-handed, while the other amphiphiles assembled into flat ribbons alone or co-existing with helices.[59,60]

The chirality of the assembling blocks is essential for the induction of helicity and handedness.[54] Studies with homochiral (containing either D- or L-amino acids) and heterochiral (composed by both D- and L-amino acids) synthetic peptides have determined the critical elements for induction of twist and chirality transfer from molecular to supramolecular level.[6,46,58,61–63] These studies revealed that generally, the amino acids order in the peptide chain is important for instructing a twisting of the assembled structures (*e.g.* fibres or ribbons) whereas the stereochemistry of the terminal amino acids are determinant for the handedness of the assembled helical structures (Fig. 8). It has been also demonstrated that changing the configuration of a single stereocenter can affect dramatically the morphology of the assemblies.

The helix propensity depends also from the helix length,[64] N- or C-capping,[58,65] charge,[66] side chains, among others.[66] For example, side chains/functional groups that are exposed on the surface upon assembly define the surface topology of the suprastructure and affect its handedness *via* attractive and repulsive interactions.[56,57] Recent data have demonstrated that the effect of aromatic side substituents on handedness determination is more powerful than the aliphatic counterparts.[56] The overpower effect of the aromatic side chains is due to their intramolecular steric repulsion to the monomer backbone and

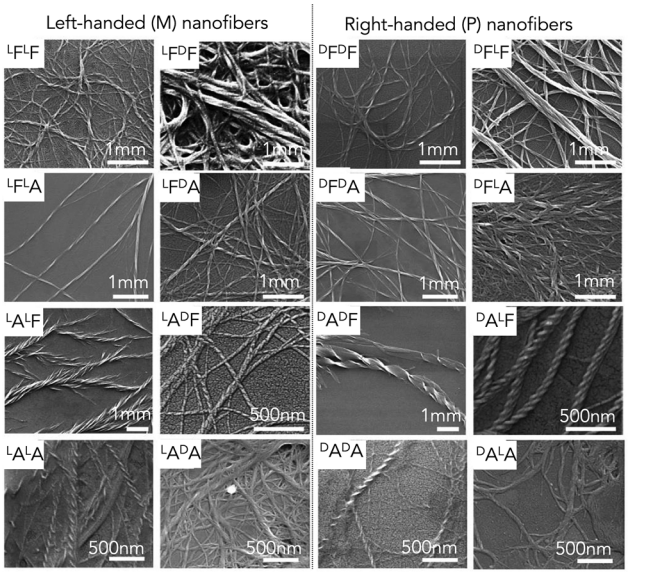

Fig. 8 Effect of amino acids stereochemistry on the helix handedness. The stereochemistry of each amino acid is shown as superscript; F: phenylalanine, A: alanine. Adapted with permission from ref. 63 Copyright 2021 by John Wiley and Sons.

Open Access Article. Published on 13 August 2025. Downloaded on 1/7/2026 10:35:48 PM.
This article is licensed under a Creative Commons Attribution 3.0 Unported Licence.

intermolecular directional aromatic stacking that induces chiral flipping between single β-strands within multi-stranded β-sheet.

Systematic studies with carbohydrates are scarce because of their challenging synthesis but also because of their complex supramolecular interactome and stereochemistry. Most studied amphiphiles contain only one or two monosaccharides conjugated to rigid aromatic or long aliphatic chains. Such carbohydrate models are oversimplified and limited when compared to natural carbohydrate systems (*e.g.* polysaccharides, glycosaminoglycans) as well as to the available peptide models. As an example, they do not provide information about the influence of monosaccharides order in the monomers on the supramolecular organisation, helicity and handedness. Interestingly, there is a significant body of studies devoted to the effects of the length and structure of the aromatic/aliphatic portion of the amphiphiles on their self-assembly but there are few molecular designs targeting specifically the stereochemical potential of the saccharide segment. Fuhrhop *et al.* reported on the assembly of diastereomeric and enantiomeric *N*-octyl-glyconamides.[26,54,67] They have observed that the chirality of the helices is predetermined by the chiral monomers, *e.g.* left-handed twisted ribbons were assembled from *N*-octyl-D-galactonaminde, while right-handed twisted ribbons were formed from the L-isomer (Fig. 9a).[26]

However, not all D-isomers form left-handed twists, *e.g.* *N*-octyl-D-gluconamide assembles in right-handed helices with diameter of 120 Å and pitch height of 200 Å (Fig. 9a).[60] Crystallographic studies have shown V-like conformation for the gluconamide (with bending at C1) that is essential for the arrangement in head-to-tail monolayers and their bending towards formation of helices (Fig. 9b).[60] Recently, we have reported helical assembly of amphiphiles, in which the carbohydrate is in its hemiacetal form and is functionalised with aromatic Fmoc group (Fig. 9c).[52] In these amphiphiles the supramolecular interactome is different: Fmoc functionality allows for intermolecular π–π stacking as well as for intra- and intermolecular CH–π stacking with the hemiacetal ring (Fig. 9c).[9,50] We have compared epimers that differ by the stereochemistry of C4. This small structural difference results in the formation of two CH-planar faces (C1–C3–C5 and C3–C4–C5) *via* which the galactose amphiphile can participate in CH–π interactions, and as a consequence, it assembled in either left- or right-handed helices (interconversion polymorphs). In comparison, the glucose has only one CH-planar face (C1–C3–C5) and formed only right-handed helices.[52] Delbianco *et al.* have used aromatic amphiphiles in which the carbohydrate moiety is made of disaccharides and reported similar twisting tendency but the generated assemblies are bigger.[11]

Bolaamphiphiles with aromatic core substituted with mono- and disaccharides have been also studied as monomers for helical self-assembly (Fig. 10).[69,70] Functionalisation with carbohydrates enhances the solubility of the amphiphiles and add chiral elements that promote helical organisation while the aromatic core allows for π-stacking. An important feature of these helices is the surface exposure of carbohydrates (Fig. 10a) that makes them available for interactions with proteins.[70]

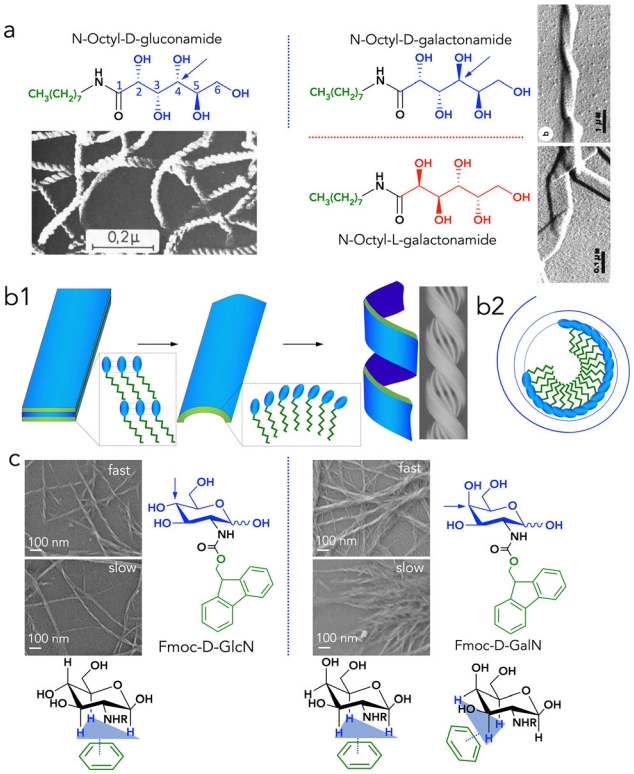

Fig. 9 Examples of supramolecular helices assembled from carbohydrate amphiphiles (a) different *N*-octyl-glyconamides (open-chain carbohydrate) assemble in distinct helical structures. SEM images are reproduced with permission from ref. 59 for *N*-octyl-D-glucosamide Copyright 1985 by Elsevier and ref. 26 for the *N*-octyl-galactonamides Copyright 1988 American Chemical Society. (b) Mechanisms for the formation of helical assemblies *via* (b1) twisting of planar sheets and (b2) bending and fusion of micelles. The 3D reconstruction of the 6-bilayer helix in (b1) is reproduced with permission from ref. 68 Copyright 1996 by Elsevier. (c) Epimers of aromatic *N*-glycosamines (different stereochemistry at C4, blue arrows) assemble in helices that are different from the open-chain carbohydrate amphiphiles due to the divergent supramolecular interactome and depend on the colling rate (fast and slow). Images are reproduced from ref. 52 Copyright 2024 Royal Society of Chemistry. Stereoisomers are separated by dashed lines (blue for epimers and red for enantiomers).

Besides these examples, systematic studies about chirality propagation from molecular to supramolecular level with carbohydrates are still scarce: the assembly of carbohydrates containing longer sequences, and heterochiral saccharides is still enigmatic. However, few recent reports demonstrate the power and great potential of the stereochemical wealth of carbohydrates in synthesis of foldamers and promise exciting new breakthroughs.[53,71,72]

The geometry of the monomers also influences the formation of helices and their handedness.[23,54,67] Changes in molecular geometry affects the orientation of H-bond donors and acceptors, rigid backbones, or planar aromatic rings that are important for the stacking and the formation of a helical structure. According to molecular geometry, different helix propensity of the naturally occurring amino acids in proteins has been determined with alanine favouring the formation of α-helices and proline breaking the helix formation because of its

 This journal is © The Royal Society of Chemistry 2025

Open Access Article. Published on 13 August 2025. Downloaded on 1/7/2026 10:35:48 PM.
This article is licensed under a Creative Commons Attribution 3.0 Unported Licence.

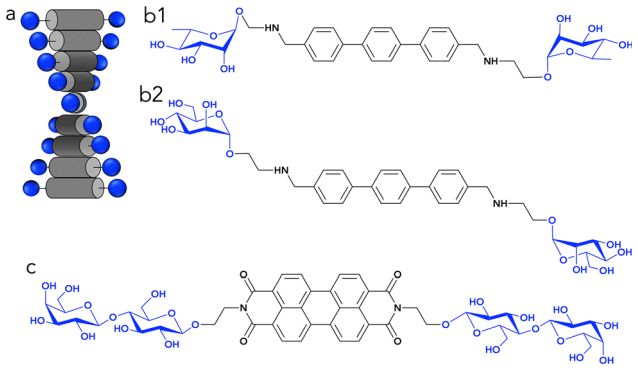

Fig. 10 (a) Schematic presentation of helical self-assembly by π-stacking of the carbohydrate bolaamphiphiles with aromatic core. (b) and (c) Examples of carbohydrate bolaamphiphiles, which assemble into helices in aqueous environment: (b) terphenyl bolaamphiphiles of (b1) α-L-rhamnopyranose and (b2) α-D-mannopyranose assemble in helices with opposite handedness;[69] (c) D-lactose functionalized perylene bisimide derivative assemble into right-handed supramolecular helix.[70]

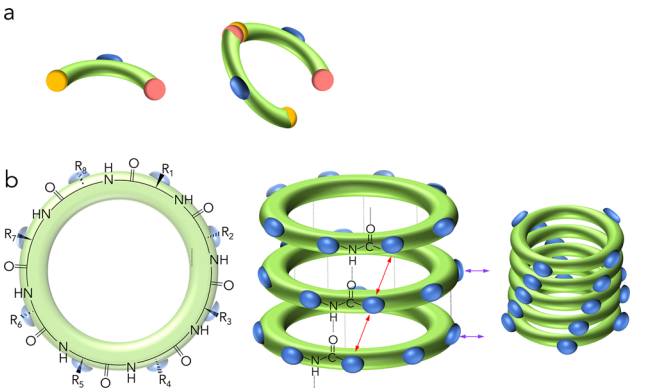

Fig. 11 Schematic presentation of the polymerisation of (a) helical and (b) cyclic peptides towards supramolecular helices. The repulsive/attractive forces between the side chains (red arrows) influence the helix properties (*e.g.* radius of curvature and gradient angle), as well as the following hierarchical organisation of the helices (purple arrows).

rigid ring structure, absence of a hydrogen at the amide nitrogen (preventing H-bonding), and its fixed conformation, which is incompatible with the helical geometry.[73] The diverse helical conformations in proteins are illustrative for the importance of the molecular geometry. The α-helix (backbone torsion angles $\varphi = -57^\circ$ and $\psi = -47^\circ$) is the most stable one.[74,75] The stability is due to the optimal side chain packing resulting from the H-bonding between each –NH group from the backbone and the –C═O group that is at four positions distance ($n + 4$) in the backbone. The α-helix contains 3.6 residues per turn, has a pitch of 5.4 Å, and a strong dipole moment due to the alignment of –C═O groups along the helix axis. In 3_{10} helix, the H-bonding is between –NH and –C═O that is 3 positions apart (n + 3) resulting in a tinner (3 residues per turn) and more elongated (5.8–6 Å) helix when compared to α-helix.[75] The dipole moment is decreased because the –C═O groups are tilted off the helix axis and the overall geometry leads to shorter and less stable helices (typically found at helix termini or as short segments). The π-helix is wider and looser than both α- and 3_{10}-helices (4.5 residues per turn and H-bonding between –NH and –C═O groups that are 5 positions apart). The π-helices are conformationally diverse (broad range of torsion angles have been reported) and can introduce significant local distortion or bends in the helix. Finally, in proline helices that are frequently found in collagen the regular H-bonding is impeded – proline introduces kinks, distortions or breaks, thus, increasing the structural flexibility.[76] An example is the polyproline II helix that has an open, left-handed, extended structure with 3 residues per turn and no internal H-bonds.

From a molecular geometry perspective, helical and cyclic peptides (peptides where the amino and carboxyl termini are linked) seem the straightest monomers for formation of supramolecular helices (Fig. 11).[77,78] Their main advantages are the predictable geometry defined by the narrow range of energetically favourable combinations of torsion angles and well-understood sequence-to-structure relationships that allow polymerisation towards targeted oligomeric states and topologies.[79]

In the case of helical peptides, the assembly is usually in head-to-tail fashion (Fig. 11a),[80] while the assembly of cyclic peptides is usually driven by formation of multiple-hydrogen-bonding arrays and side chain-driven aggregation (Fig. 11b).[81]

The most robust and widely used design relies on cyclic peptides with an even number of alternating D- and L-amino acids. This arrangement promotes a flat, planar ring conformation where all amide –NH groups point in one direction and all –C═O groups in the opposite, enabling strong, directional intermolecular H-bonding upon stacking (Fig. 11b). Cyclic β-peptides, cyclic α,γ-peptides, and cyclic peptides containing ε-amino acids are also used in some approaches. The stereochemical restrictions imposed by the design of plane molecular cycles limit the choice of the isomers that can be used and thus, the stereochemical information that can be coded. This drawback can be partially overcome by specific design of the side chains – while the backbone H-bonding is the primary driver of the assembly, side chain interactions (*e.g.* hydrophobic, hydrophilic, aromatic stacking) can control lateral aggregation, solubility, and functionalisation. For example, amphiphilic designs can promote bundling or control the orientation of the assemblies in water.[82] There are several recent reviews about these peptides that describe in detail the molecular design, the symmetry restrictions and the assembly in supramolecular helices.[75,77,80,83,84]

Design of higher order structures such as coiled coils is related with the transfer of chirality to higher structural levels. The hallmark of coiled coils is the seven-residue (heptad) repeat with alternating hydrophobic and polar residues HPPHPPP, (H and P represent hydrophobic and polar residues, respectively) denoted as a-b-c-d-e-f-g (Fig. 12a). The alternation of hydrophobic and hydrophilic residues creates an amphipathic α-helix. The side chains at the (a) and (d) positions from one helix fit into the spaces (holes) formed by the side chains of another, stabilizing the structure through ''knobs-into-holes'' packing.[85] Aromatic residues (Phe, Trp, Tyr) are generally avoided at these positions due to steric constraints and bulkiness, which can destabilize the core. Positions (e) and (g) are

Open Access Article. Published on 13 August 2025. Downloaded on 1/7/2026 10:35:48 PM.
This article is licensed under a Creative Commons Attribution 3.0 Unported Licence.

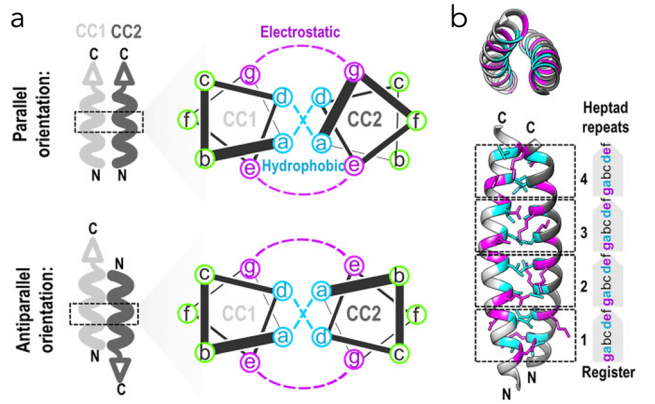

Fig. 12 Self-assembly of coiled coils by peptides. (a) Essential heptapeptide sequence contains hydrophobic amino acids in positions a and d (cyan) and charged amino acids in g and e positions (magenta) allowing formation of parallel and antiparallel heterodimers. (b) Schematic presentation of the structure of a parallel heterodimer, in which the residues involved in electrostatic and hydrophobic interactions are coloured magenta and cyan, respectively. The image is reproduced from ref. 87 under CC BY 4.0.

usually occupied by charged residues (*e.g.* Glu, Lys, Arg), which can form interhelical salt bridges that stabilize the assembly and determine specificity (Fig. 12b): oppositely charged residues promote the pairing (positive design), while similar charges can prevent undesired associations (negative design). The other positions (b, c, and f) are solvent/interface exposed and can be designed to tune the helical propensity and favour the formation of dimers, tetramers, or higher-order oligomers.[86]

Peptides can be engineered to be orthogonal, *i.e.* assembling only with their designated partners, or flexible linkers can be used to connect multiple coiled-coil domains in more complex assemblies.[88] Collagen triple helices have been used as model to develop synthetic higher-order mimics but achieving self-assembling control similar to that in natural α-helical coiled coils remains challenging due to the limited understanding of the sequence–structure relationship in collagen higher-order assembly.[89,90] Further information about the assembly of coiled coils can be found elsewhere.[91–93]

4.2. Environmental factors

Recent studies have demonstrated that, in aqueous environment, supramolecular polymerisation can involve large kinetic barriers and instead of thermodynamically stable products (SP2, Fig. 13), formation of kinetic products (SP1, Fig. 13) occurs.[20,94,95]

Such kinetically-driven pathways/products are often observed in living systems and important for self-organisation of life and evolution.[95] The stability of the kinetic products depends on the magnitude of the energy barrier(s): at low $\Delta E_A \approx k_0T$ metastable products are formed that are transitional and transformable in more stable products within the reaction time, while kinetically trapped products obtained at higher $\Delta E_A \gg k_0T$ can be transformed into thermodynamically stable products only upon external stimulus. Of note, when the

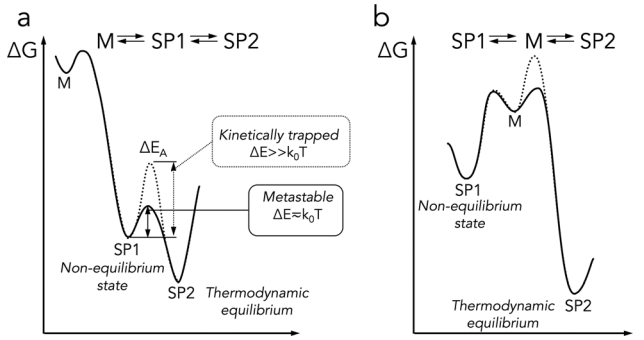

Fig. 13 Schematic presentation of (a) consecutive and (b) competitive pathways of supramolecular polymerisation of monomers (M) that can result either in kinetic supramolecular product (SP1) or in stable thermodynamic product (SP2).

reaction follows the competitive pathway (Fig. 13b), the transformation of kinetic products into thermodynamic one is only possible *via* disassembly and *de novo* assembly. In any case, the common outcome is polymorphism (existence of systems with different morphologies and chirality from the same monomers) that can be controlled by the used conditions, *e.g.* solvent composition, temperature, and pH (Fig. 14).[4,96–99] The physiological importance of this process is well documented for proteins/peptides that can fold in different conformations and chirality (Fig. 1c), *e.g.* different polymorphs of amyloid fibrils have different stability and toxicity.[58,96,100–102] The low energy barriers between different polymorphs allows their co-existence and interconversion but environmental factors can be used to favour the formation of one polymorph over others.

4.2.1. Solvent. Solvent is an important player in the self-assembly process: its polarity, viscosity, and chirality affect the supramolecular packing, as well as the thermodynamic and kinetic parameters of the nucleation and elongation

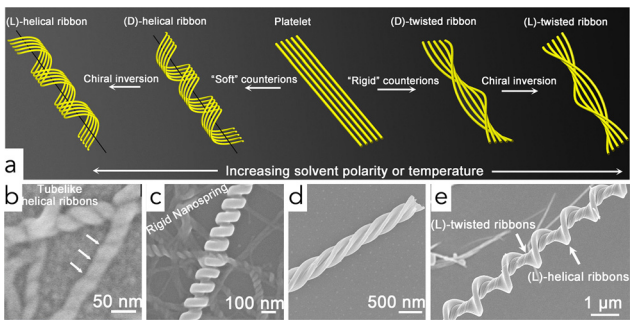

Fig. 14 Polymorphs of ferrocenediphenylalanine (Fc-FF, 4 mM) helical assembles obtained at different conditions. (a) Schematic presentation of Fc-FF self-assembly in which each yellow line represents a simplified strand of a β-sheet. (b)–(e) SEM image of (b) the tubelike helical ribbons (10% 2-propanol and 90% PBS solution 100 mM, pH 5.6); (c) nanospring (10% 2-propanol and 90% H_2O, pH 5.6 (20 mM ethylenediamine), 37 °C); (d) nanohelix formed through the helical twisting of two crossed ribbons (10% HFIP and 90% H_2O, pH 6.0 (20 mM piperazine), 37 °C); (e) nanoscrew formed through a combination of the two elementary forms of β-sheet arrangement (10% acetonitrile and 90% H_2O, pH 5.6 (20 mM piperazine), 50 °C). Reproduced from ref. 98 with permission from American Chemical Society, copyright 2015.

This journal is © The Royal Society of Chemistry 2025

Open Access Article. Published on 13 August 2025. Downloaded on 1/7/2026 10:35:48 PM.
This article is licensed under a Creative Commons Attribution 3.0 Unported Licence.

processes.[103] As a result, helices with different handedness and dimensions (pitch and thickness) can be generated from the same building blocks in different solvents. One example are the helices assembled from peptide amphiphiles derived from L- and D-alanines (Fig. 15a) in different solvents.[104] In water, these amphiphiles form nanoribbons whose handedness is determined by the chirality of the amino acid at the C-terminus (Fig. 15b). Similar nanoribbons are assembled in THF but their handedness is opposite (Fig. 15c). SAXRD patterns showed the formation of a lamellar structure in either solvent that is due to the hydrophobic stacking between the alkyl chains (Fig. 15d).

However, the interlayer distance (*d*-spacing) between these chains in water is shorter than in THF showing different packing in these solvents. This difference can be explained by the different affinity of the amphiphile units to these solvents – the peptide can form H bonding with water while the alkane portion has higher affinity to THF. The *d*-spacing is not compatible with the intercalation of the THF between the bilayers and thus, the packing can be explained with an inversion of the handedness in this solvent (Fig. 15d) that is confirmed by microscopy observation.

In synthetic systems, a solvent switch method is commonly used to trigger the self-assembly. This method consists of dissolving the amphiphiles in a good solvent followed by the addition of a second, usually poor solvent. In the case of supramolecular materials for bioapplications, the choice of solvents is quite limited due to the toxicity of most organic solvents: DMSO is commonly used as a good solvent because of its low toxicity and ability to dissolve both polar and nonpolar compounds, and water is added as a co-solvent to trigger the assembly. Water can participate in H-bonding either as a donor or an acceptor and several studies have shown that its amount can affect the stacking and packing.[62,105,106]

4.2.2. pH. pH is an important factor from the bioapplication point of view because different physiological and pathological processes are associated with changes of local pH. For example, the pH is an important factor in wound healing: acidic pH promotes the healing and this effect is related with conformational changes in overexpressed proteases, which results in a decreased activity.[107] Thus, the possibility to control the helix formation, handedness and stability *via* pH adjustment is of great interest.

pH change can alter the protonation state of functional groups, thereby influencing the supramolecular interactome and the assembly process – it can result in morphological changes or in the inversion of handedness.[62,108] The pH effect is most pronounced for helices whose assembly is driven by electrostatic interactions. One example is the co-assembly of chiral phenylalanine amphiphiles and achiral cationic poly(acrylamide-*co*-diallyl dimethylammonium chloride) (CPAM, Fig. 16a). At neutral pH, the D- and L-isomers of the amphiphile assemble into helices with opposite handedness that are stabilized by electrostatic interactions with CPAM (Fig. 16b).[109] At basic pH (pH 10), this handedness is preserved but at acidic pH the handedness is inverted and the assembled helices are not exact mirror images. The reason for these changes is the different supramolecular interactome involved in the assembly: at acidic conditions there are mainly

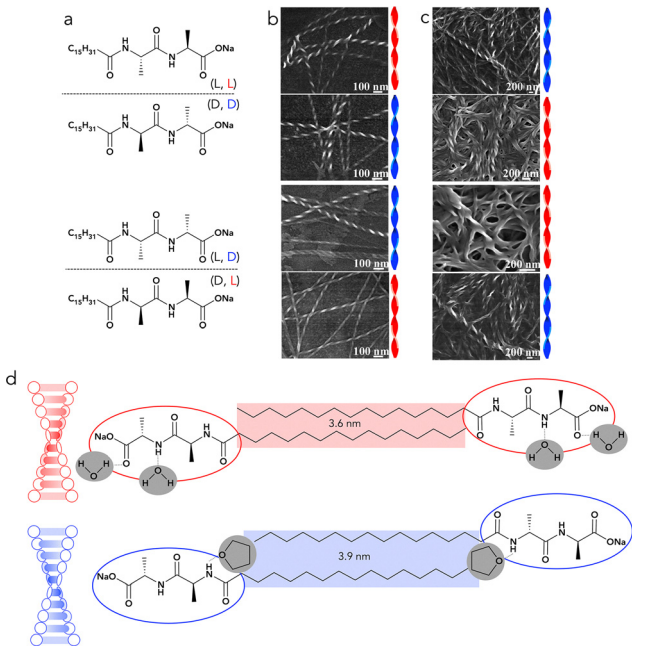

Fig. 15 Effect of the solvent on the handedness of supramolecular helices: (a) chemical structures of peptide amphiphiles used for the assembly of helices in (b) aqueous solutions at concentrations of 2.0 g L^{-1} and in (c) THF at concentrations of 30 g L^{-1}. (d) Schematic presentation of the solvent effect on the molecular packing and handedness of helices assembled from the L,L isomer based on the SAXRD data. Adapted from ref. 104 with permission from American Chemical Society, Copyright 2013.

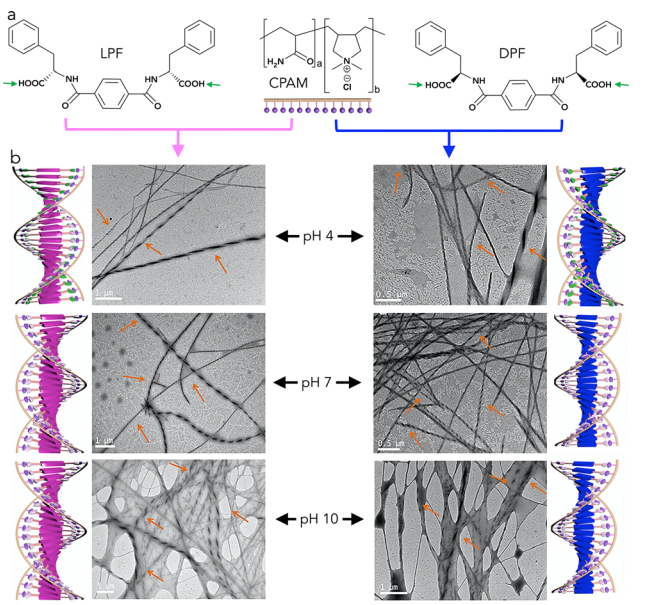

Fig. 16 (a) Chemical structures of chiral phenylalanine amphiphiles and achiral cationic poly(acrylamide-*co*-diallyl dimethylammonium chloride) and (b) schematic presentation and TEM images showing the co-assembly and the inversion of the handedness at different pH. Ionizable groups are indicated in green. Adapted with permission from ref. 109 with permission from Elsevier, Copyright 2019.

Open Access Article. Published on 13 August 2025. Downloaded on 1/7/2026 10:35:48 PM. This article is licensed under a Creative Commons Attribution 3.0 Unported Licence.

hydrogen bonds between the carboxyl groups of the amphiphiles and the amides of the CPAM, while at the basic pH the carboxyl groups are ionized and interact with cationic quaternary ammonium ion through electrostatic interactions, resulting in rearrangement and different packing.[109]

The effect of pH on packing can result not only in changes of helices handedness, pitch and thickness but also in transition to completely different morphologies. This is the case of chiral Fc-FF assembled in 2-propanol/water (1/9) that in very narrow pH range change from nanospheres (pH > 5.9) to nanohelices (pH 5.7–5.9) and nanobelts (pH 5.5).[62]

4.2.3. Temperature. The effect of the temperature can be different – from fine tuning of helices properties such as pitch, diameter, handedness to formation of assemblies that are with completely different morphologies.[98,110] For example, tunning of the temperature allows precise control of the diameter and helical pitch of the self-assembled chiral nanostructures by balancing the chiral interactions and the geometric constraints as shown for Fc-FF (Fig. 17).[98]

In fact, the temperature change is a common method to induce assembly: cooling down a warm solution of monomers is often used not only to overcome their limited solubility but also to direct and control the assembly. Of note, in temperature-induced assembly, the final temperature is important but also are the cooling rate and the cooling profile/thermal history that can be tuned to selectively obtain different assemblies.[52,111–114] We and others have shown that the cooling rate can be used to control the handedness of the helices assembled from carbohydrate amphiphiles.[52,112] The aromatic amphiphile of D-galactosamine (*N*-fluorenylmethoxycarbonyl-D-galactosamine) assembles into P-helices upon fast cooling (40 K min^{-1}) and into M-helices upon slow cooling (5 K min^{-1}) in water (Fig. 9c).

The inversion between left- and right-handed states is governed by an energy barrier(s), with one state being kinetically trapped and the other thermodynamically stable (Fig. 13).[58] A slow cooling rate allows overcoming the kinetic barriers and promotes well organized, high-fidelity self-assembly ultimately resulting in thermodynamic products – stable, lower-energy structures. On the other hand, a fast-cooling rate can trap the system in a metastable state or produce kinetically controlled structures, *i.e.* it can result in intermediate or less ordered structures that might be less stable over the time. An illustrative example for the balance of different interactions under kinetic and thermodynamic control is the co-assembly of chiral phenylalanine amphiphiles (LPF and DPF, Fig. 16a) and achiral naphthylamide derivatives upon temperature or a solvent switch.[113] Thermodynamically stable non-helical belts and sheets are obtained upon temperature decrease due to the non-helical π–π stacking between the achiral pyridine derivatives that occurs first followed by H-bonding of the phenylalanine blocks (Fig. 18a).

The solvent switch method, on the other hand, results in the formation of kinetically trapped chiral structures such as helical ribbons, twists, superhelices and double helices because at these conditions H-bonds between the chiral and non-chiral components are formed first leading to the chirality transfer and then these chiral co-assembled blocks are packed into helical structures (Fig. 18b).[113]

Temperature change can also induce disassembly or results in a different packing/morphology (*e.g.* micelles, vesicles) if the helical system is a kinetic product (Fig. 13). Such thermoresponsiveness can have different biomedical applications. For example, D- and L-forms of alanine-functionalized phenyleneethynylenes have been used as templates for chiral plasmons.[115] In this approach, gold nanoparticles are grown on chiral templates assembled from the amphiphiles. Then, the templates are dissociated upon increasing the temperature, resulting in free-standing chiral plasmonic nanostructures, in which the nanoparticles keep the helical organisation, and the handedness induced by the templates.

4.2.4. Other environmental factors. Other environmental factors such as amphiphiles concentration, presence of counterions, ionic strength, and application of stimuli such as ultrasound and photoirradition, can be also used to induce supramolecular chirality and control the handedness of the assemblies.[52,98,116,117]

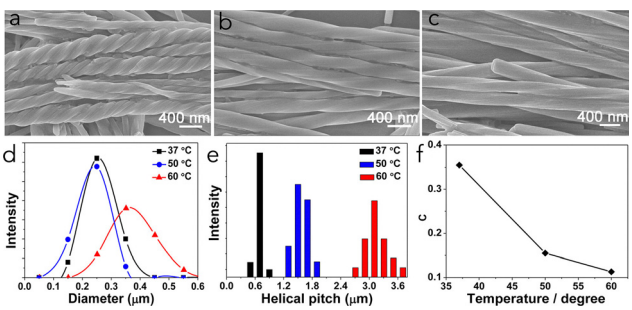

Fig. 17 Effect of the temperature on the morphology of helices assembled from ferrocenediphenylalanine (Fc-FF) at (a) 37 °C, (b) 50 °C, and (c) 60 °C. (d) Diameter (*D*) and (e) helical pitch (*H*) distributions of the helices formed at different temperatures. (f) Profile of the *C* values as a function of temperature, where C=D/H. Adapted from ref. 98 with permission from American Chemical Society, Copyright 2015.

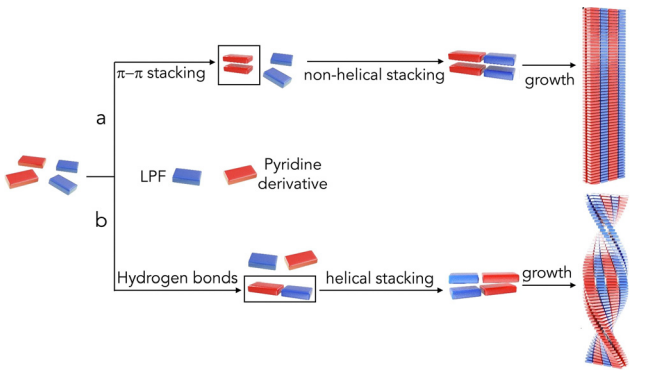

Fig. 18 Schematic illustration of the supramolecular interactions involved in the formation of (a) thermodynamically stable assemblies upon temperature decrease and (b) kinetically trapped products upon solvent switch. Adapted from ref. 113 with permission. Copyright 2022 John Wiley and Sons.

This journal is © The Royal Society of Chemistry 2025

Open Access Article. Published on 13 August 2025. Downloaded on 1/7/2026 10:35:48 PM. This article is licensed under a Creative Commons Attribution 3.0 Unported Licence.

5. Bioapplications of supramolecular helices

Helical supramolecular systems have been developed as fundamental tools aiding the understanding of homochirality in living systems but also as means to manipulate the chirality-sensitive processes such as proteins folding and aggregation, proteolytic stability, cells apoptosis, bacterial adhesion.[118–120]

5.1. Self-replicating systems

Self-replicating systems aim to explain the emergence of life by providing pathway(s) for transferring structural information, variation, and evolution in prebiotic environment without the need of complex replication biomachinery, *i.e.* they provide information about the synthesis of life from non-living matter.[121,122] The first self-replicating peptide system was reported in 1996[29] and since then this research area has attracted great attention. In this study a template-assisted mechanism is reported – the targeted peptide (template) catalyses its own formation from two shorter ones in aqueous solution by stabilising the assembly of the fragments and accelerating their ligation. The replication showed parabolic but not exponential growth due to product inhibition caused by the dimerization of two templates. Recently, Otto *et al.* reported supramolecular polymerization-driven self-replication (Fig. 19a).[31,123,124] The process takes place in a mixture of interconverting peptides leading to the autocatalytic sequestration of the assembling molecules and causing their exponential self-replication (Fig. 19a).[31,123] After the new peptide is formed, it can dissociate from the original template and catalyse the formation of more copies, leading to a cycle of self-replication. Such system was used to demonstrate the effects of chirality on self-replication (Fig. 19b).[125] Systematic studies allowed to select a replicator that incorporates material of its own handedness from a racemic mixture of precursors, resulting in stereochemical sorting of the precursors into enantiopure replicators. The enantioselectivity of this system depends on the ring size of the replicator that appear to impose constraints on its supramolecular organization.

So far, no purely carbohydrate-based self-replicating systems are known but self-replication involving carbohydrates does occur in certain chemical systems. The best-known example is the formose reaction – self-replicating network in which simple carbohydrates are generated from formaldehyde but the carbohydrate generation is not template-assisted.

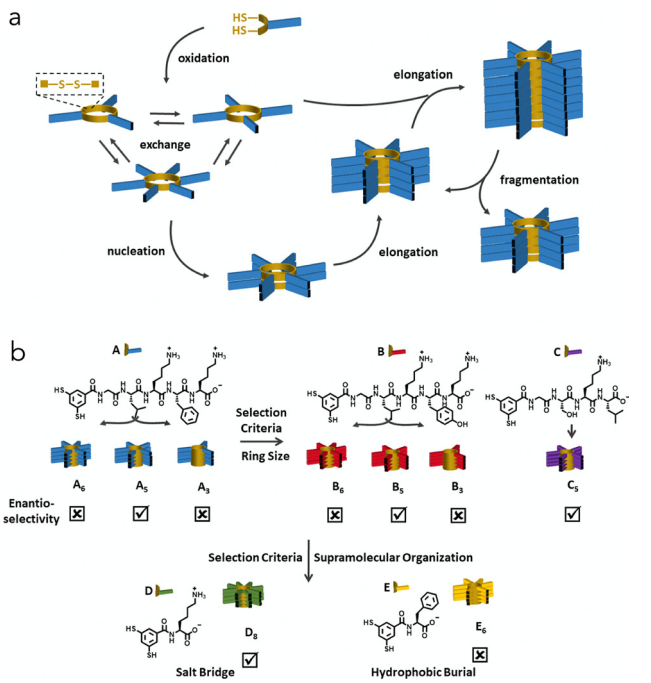

Fig. 19 Example of self-replicating peptide system. (a) Building blocks consisting of a peptide strand (blue) attached to a dithiol aromatic group (yellow) oxidize in aqueous medium to form cyclic oligomers linked through disulfide bonds. The macrocycles constantly exchange in the presence of an unreacted monomer. One macrocycle of a specific size (here it is a hexamer) can stack to form a nucleus, which then grows into a fibre by incorporating material from smaller macrocycles (elongation). (b) Replicators made from different peptides (A, B, C, D, or E) show enantioselectivity (*i.e.*, incorporation of only one enantiomer into a single fibre) that depends on the ring size and the possible interactions conferred by their respective peptide strand. The image is reproduced from ref. 125 under CC BY 4.0.

5.2. Amyloid-like fibres

Amyloid-like fibres are subject of extensive research in disease and material science contexts. This interest is fuelled on one hand by their pathological role in different neurodegenerative diseases, including Alzheimer's disease, Parkinson's disease, type II diabetes, and on the other hand, by the possibility to tune their properties by environmental factors.[102,126–128]

Amyloid-like fibres are formed by proteins or peptides that misfold and aggregate into typical cross-β sheet structure, in which β-strands align perpendicular to the fibre axis, giving the fibres their characteristic stability and strength.[127,129,130] Analysis of different polymorphs have shown that the helical morphology of the fibres is due to the chirality of the building blocks and that generally the helical pitch of the fibrils increases with the width (Fig. 1c).[102]

Different studies have shown that right-handed amyloid assemblies are implicated in Alzheimer's disease and exhibit a higher resistance to proteinase K degradation when compared to their left-handed counterparts.[58,96] From a disease control perspective, chirality has been explored to inhibit amyloid β growth, elongation, aggregation, and recognition. The use of non-canonical D-amino acids instead of the natural L-analogues showed that the assembly process differs for the stereoisomers and the properties of the aggregates are distinct.[131–133] Dutta *et al.* demonstrated that the cellular uptake of amyloid β is a stereoselective process with a preference for the natural L-isomer (5-fold higher than D-isomer).[132,133] Such preference can explain the higher toxicity of the L-isomer and suggests receptor-mediated internalisation in which the aggregates are recognised and bound with a certain degree of stereoselectivity. Moreover, supplementation of the D-isomer reduces the concentration of toxic oligomers from canonic L-peptide formed *in vitro*, while the racemate accelerates the fibrils formation.[133] Peptide sequences that

Open Access Article. Published on 13 August 2025. Downloaded on 1/7/2026 10:35:48 PM. This article is licensed under a Creative Commons Attribution 3.0 Unported Licence.

contain symmetry breaking amino acids (see Section 4.1) have been also explored as amyloidosis inhibitors. In particular, the tripeptide $^{L}P^{D}F^{L}F$ disturbs the β-sheet organisation and showed promising inhibitory effect *in vitro*. *In vivo* studies have also explored this approach.[106,134] Gold nanoparticles functionalized with L- and D-glutathione (contains G that has low helix propensity due to its small size, which allows high flexibility and polar C that typically do not favour helices) crossed the blood–brain barrier and the D-construct had stronger inhibitory effect, decreased amyloid β plaque deposition in the brain, and rescued the memory deficits of Alzheimer's Disease mice.[134]

5.3. Effect on cell behaviour

Chiral recognition is in the basis of cell signalling and affects cells fate.[7,118,135–143] Several studies have shown that the incorporation of D-amino acids in the self-assembling peptide sequences reduces the toxicity of supramolecular helices towards different cells.[141,142] A possible cause for this effect is the lower affinity that the nanohelices assembled from peptide amphiphiles with D-amino acids have for lipid bilayers (*i.e.* cell membrane) compared to the ones with L-amino acids.[142] Another reason is a distinct protein interaction with helices with different handedness.[138] Feng *et al.* used a series of PF derivatives and showed that left-handed (M) nanofibres (Fig. 20a) have stereoaffinity to native protein molecules and provide more integrin-binding sites for cell adhesion and spreading when compared to right-handed (P) nanofibres (Fig. 19b). Consequently, the M nanofibres promote cell spreading, proliferation (Fig. 20d–g), and cell differentiation.[135,144] Of note, this effect has been observed for either left-handed nanofibres assembled from peptide amphiphiles containing L- (Fig. 20g) or D-amino acids.

An opposite effect has been observed for retinal progenitor cells and helices assembled from L- and D-phenylalanine derivatives: right-handed nanofibres assembled from the D-enantiomer promote cell neuronal differentiation, whereas left-handed fibres decrease this effect.[139] The results are explained by the stereoselective interaction between the helices and retinol-binding protein 4 that is a main player in the retinoic acid metabolic pathway. The same helical systems have been also used to direct the differentiation of mesenchymal stem cells and showed that the left-handed helices enhance the osteogenesis, while right-handed helices promote adipogenesis.[140] This chirality dependent lineage commitment is due to the stereospecific clustering of the mechanosensor Itgα5 by the left-handed helices.

Altogether these data demonstrate that helical nanostructures can be used to strategically hinder (burying in the helix cavity) or expose bioactive sequences that target specific receptors and downstream signalling pathways, thus, providing efficient tools for biogenesis and regenerative therapies. The manipulation of cellular chiral environment by the supplementation of supramolecular helices can also direct the cellular response because enzymes have less tolerance towards D-amino acids – the incorporation of even a single D-amino acid in self-assembling peptide sequences is enough to slow down its enzymatic recognition and transformation.[145]

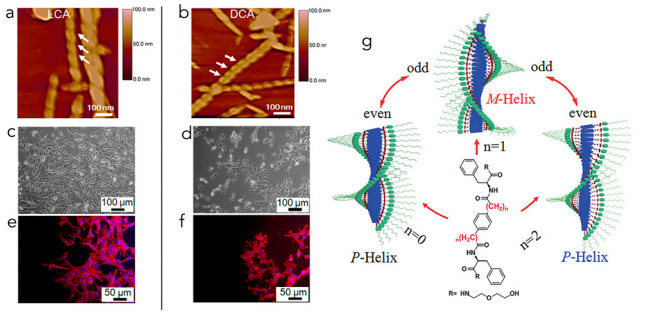

Fig. 20 Effect of handedness of supramolecular helices on the cell adhesion. (a) and (b) AFM images of (a) left- (M) and (b) right-handed (P) helices assembled from PF derivatives (as the ones presented in Fig. 14a, for which the COOH group is esterified); (c) and (d) optical and (e) and (f) fluorescence microscopy images of NIH-3T3 cells after 5 days of culture on films from the respective enantiomers. Adapted with permission from ref. 138 Copyright 2019 American Chemical Society. (g) Chemical structure of L-PF derivatives and illustration of helical chirality inversion tuned by the number of the methylene units. Adapted with permission from ref. 135 Copyright 2018 John Wiley and Sons.

5.4. Antibacterial applications

Chirality plays a fundamental role in bacterial physiology, affecting the structural integrity and the interactions of bacteria with their environment. The bacterial cell wall is built from peptidoglycans, some of which contain D-amino acids that are crucial for the strength and rigidity of the wall and enhance the bacterial resistance to proteolytic degradation as most proteases are stereospecific and target L-amino acids. Chirality is also important for the quorum sensing – some bacteria use autoinducers with specific chirality that is essential for the interactions with the targeted receptors. Thus, any disruption in the homeostatic chirality can affect bacterial survival and functionality. Therefore, many antibiotics target bacterial structures or enzymes that are chiral. For instance, penicillin inhibits the synthesis of bacterial cell walls by interfering with enzymes that recognize D-alanine.

The interest in helical structures with antibacterial activity dates back in 1941 when the gramicidin (also known as gramicidin D) was isolated from *Bacillus brevis*. Gramicidin is a mixture of polypeptides with ionophoric properties that effectively kills Gram-positive bacteria. Its major component, gramicidin A, was the first antibiotic manufactured commercially. It is a decapenta peptide composed of alternating D- and L-amino acids (primary structure $HCO^{L}VG^{L}A^{D}L^{L}A^{D}V^{L}V^{D}V^{L}W^{D}L^{L}W^{D}L^{L}WNHCH_2CH_2OH$) allowing the adoption of a helical conformation stabilized by β-sheet type H bonding (Fig. 21a). It acts *via* so-called barrel-stave mode – gramicidin A helices penetrate the bacterial membrane where it assembles into head-to-head dimers that are enough long to span cellular lipid bilayers (Fig. 21b) and form channels *via* which small ions (H+, K+, Na+) can diffuse unregulated. The loss of ion balance causes depolarisation of the bacterial cell membrane and impairs ATP synthesis, halts bacterial cell growth, and leads to cell death. Gramicidin A clinical use is however

 This journal is © The Royal Society of Chemistry 2025

Open Access Article. Published on 13 August 2025. Downloaded on 1/7/2026 10:35:48 PM.
This article is licensed under a Creative Commons Attribution 3.0 Unported Licence.

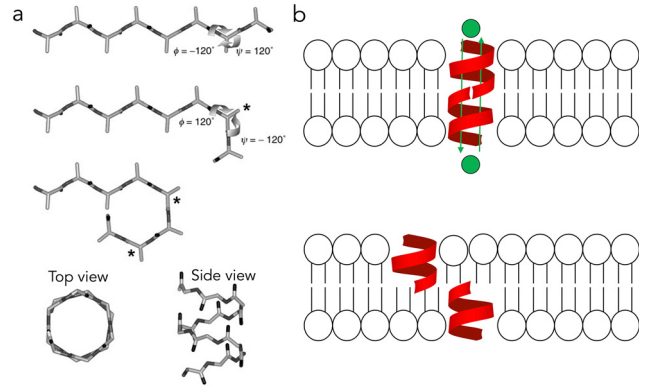

Fig. 21 (a) Effect of amino acids chirality on the peptide conformation: in all-L peptide the pleated β-conformation has $\phi = -120°$ and $\psi = 120°$ while in sequences that have D-residues (marked with asterisks) the dihedral angles of these residues must be inverted to maintain a pleated conformation able to participate in β-type hydrogen bonding. This causes kinks and loops in the peptide chain. Peptide chains with altering D/L amino acids form a β-helix. Reproduced with permission from ref. 147 Copyright 2001 John Wiley and Sons. (b) Schematic presentation of open (up) and closed (down) ion channels assembled from dimeric gramicidin A.

limited because of its toxicity to eukaryotic cells most probably due the common ion transport mechanism and different synthetic peptides with lower toxicity have been investigated.[146] The helical structure of these peptides aids the formation of pores or disrupting membranes, leading to antimicrobial activity.

GL13K is a cationic peptide that presents antibacterial activity based on electrostatic interactions with the bacterial membrane. Importantly, GL13K is not toxic to mammalian cells and has gained attention because of its efficacy against bacteria and biofilms – it prevents biofilm formation and disrupts existing biofilms. Studies with all-L and all-D isomers of GL13K showed that they both assemble into twisted nanoribbons, but this process is faster for the D-isomer.[148] This isomer has higher antimicrobial activity against Gram-positive bacteria than the L-isomer suggesting that the rate of the self-assembly is important for the antimicrobial activity. The properties of the assembled helices are also important. For instance, data obtained with homochiral C_{16}-$^{L}V_4{}^{L}R_4$ and C_{16}-$^{D}V_4{}^{D}R_4$ and heterochiral C_{16}-$^{D}V_4{}^{L}R_4$ peptides showed that the heterochiral isomer forms right-handed helices that are more stable and have higher antimicrobial activity than the homochiral analogues that do also assemble into helices but with larger helical pitch.[149] Different handedness can also result in different activity. LPF and DPF (Fig. 16a) modified at the COOH groups with the antibacterial 2-amino-5-methylthiazole (MTZ) or 5-amino-1,3,4-thiadiazole-2-thiol (TDZ) assemble into supramolecular hydrogels.[150] Both types of hydrogels have antibacterial activity against Gram-positive and Gram-negative bacteria but the D-enantiomer, which forms right-handed nanofibres, showed higher efficacy than the L-isomer that assembles into left-handed helical fibres. The length of the assemblies is also important – shorter fibres act by disrupting bacterial membrane integrity while longer ones agglutinate or entrap the bacteria.[151]

5.5. Other bioapplications

Carbohydrate–lectin interactions play important role in different biological processes, including cell growth, differentiation, adhesion, cancer metastasis, inflammation by bacteria and viruses, and the immune response. Lectins recognize specific carbohydrate termini and bind them into structurally defined pockets. The multivalent cooperative interactions are essential for this binding (so-called cluster glycoside effect) and thus, supramolecular glycohelices with multiple surface-exposed carbohydrates are excellent candidates to target lectins. An example is the supramolecular helix assembled from D-lactose functionalized perylene bisimide derivative.[70] The chiral monomers induce right-handed supramolecular stacking and exhibited specific binding with peanut agglutinin lectin. Carbohydrate–lectin interactions are implicated in the bacterial communication and have been targeted as a part of different antibacterial approaches. Lee *et al.* have demonstrated that self-assembled glyco-nanoribbons can be used to tune the bacterial agglutination and inhibit the bacterial motility, *i.e.* they are promising agents for pathogen capture, inactivation, and detection.[152,153] Of note, in these approaches the helical structure is not essential.

Fundamental understanding of the interplay between the peptide and carbohydrate chirality has been demonstrated by

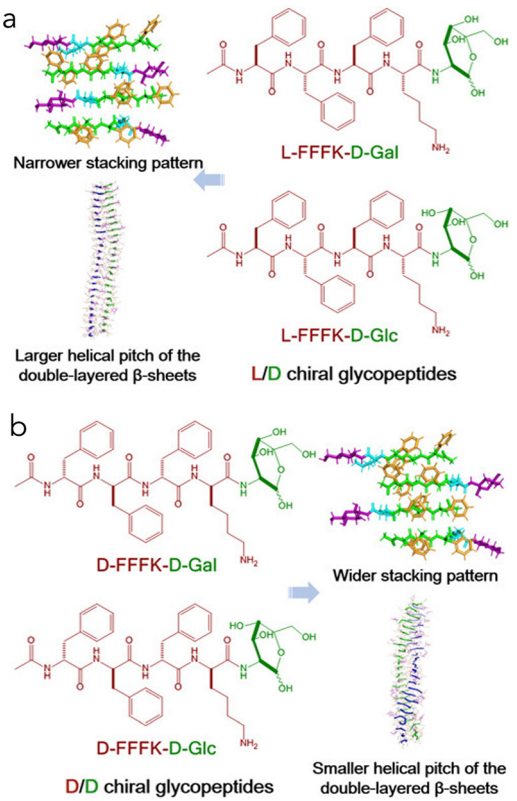

Fig. 22 Changes in glycopeptide packing arising from different chiral combinations of peptides and carbohydrates: (a) L-FFFK peptide functionalised with D-galactose (D-Gal) or D-glucose (D-Glc) and (b) D-FFFK peptide functionalised with D-Gal or D-Glc. Adapted with permission from ref. 154 Copyright 2025 American Chemical Society.

Open Access Article. Published on 13 August 2025. Downloaded on 1/7/2026 10:35:48 PM.
This article is licensed under a Creative Commons Attribution 3.0 Unported Licence.

self-assembly of glycopeptides that contain D-glucose or D-galactose unit at the C-terminus of the L- and D-FFFK.[154] The non-glycosylated peptides assembled into cylindrical nanofibres while the glycopeptides formed asymmetric helical nanostructures. L-FFFK-D-Gal exhibited a tendency to self-assemble into left-handed helices, while all other stereoisomers assembled into right-handed structures. Narrower stacking modes with augmented helical pitch were observed for the L/D glycopeptides when compared to the D/D monomers (Fig. 22). All-atom MD simulations showed that this difference is due to enhanced hydrogen bond interactions between the peptide and saccharide moieties in the L/D glycopeptides.

Recently, an assembly of macroscopic helicoids from carbohydrate amphiphiles has been reported (Fig. 23).[110,155] Because of the controlled handedness and high surface area, such structures can find applications as stereospecific templates for catalytic or enzymatic processes, as well as drug delivery systems. Yao *et al.* have studied the assembly of monosaccharide (xylose, galactose, mannose, and glucose) stearoyl esters and obtained chiral flaky microparticles only from the glucose esters (Fig. 23a).[155] Interestingly, chirality was observed only at specific α-/β-anomers ratio 20/80, while for other ratios achiral microstructures with a different morphology were assembled. The microparticles obtained from L- and D-glucose stearoyl esters had opposite helicity but the same thermal properties.

Carbohydrates have been used to instruct chirality also in co-assembly approaches. For example, bola amphiphiles containing D-glucose or D-mannose co-assemble with 1,4-benzenediboronic acid into right-handed macrohelices in alkaline aqueous solutions at temperature above 80 °C (Fig. 23b). The chirality is induced by interactions between the boronic acid and the *cis*-diols of the carbohydrate from the bola amphiphiles because in the absence of the carbohydrates non-chiral brick-shaped structures were obtained. The macrohelices emit blue luminescence and their pitch can be tuned by the selection of the monosaccharide in the bola amphiphile – when D-glucose amphiphile is used the helices have pitch of 5.4 ± 1.1 μm, while D-mannose amphiphile co-assembles into structures with pitch of 6.3 ± 1.0 μm.

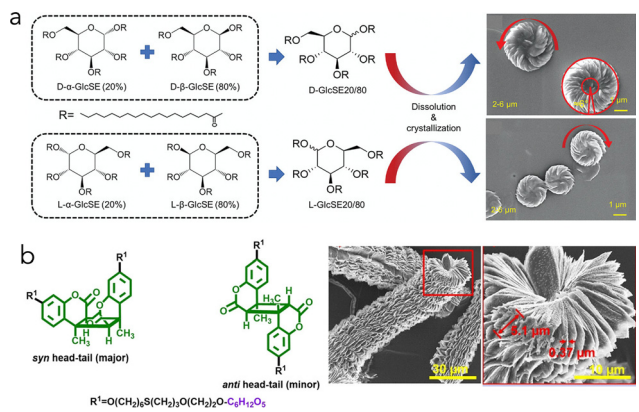

Fig. 23 Macroscopic helical structures obtained by (a) assembly of D- and L-glucose stearoyl esters (reproduced with permission from ref. 155 Copyright 2021 John Wiley and Sons) and (b) co-assembly of carbohydrate based bolaamphiphiles (in green) and 1,4-benzenediboronic acid (reproduced with permission from ref. 110 Copyright 2021 John Wiley and Sons).

Helical assemblies can be useful as templates for crystallisation of biological macromolecules or inorganic replicas. The potential of this application is underexploited and only few proof-of-concept studies have been carried.[156] The advantages in the case of proteins for example are that different active sequences can be exposed upon crystallisation on the template. Moreover, the templated structures are readily observable by microscopy and thus, can be instrumental in structure–activity studies. Inorganic helical structures are not readily prepared without template. One approach is to add the inorganic salt or oxide to the chiral organic molecules. For example, homochiral vaterite helicoids have been assembled in the presence of nonracemic mixtures of L- and D-enantiomers of amino acid (aspartic acid).[157] In another approach, the inorganic crystals are grown on previously formed helical assembly. This approach was applied for controlled growth of gold nanoparticles on supramolecular helical templates that can be used as chiroptically active materials.[158]

6. Conclusions and future trends

During the last decade, a significant advance in the elucidation of structural and environmental factors that influence the supramolecular chirality and trigger helical development has been made. Synthetic homo- and heterochiral peptides build from D- and L-amino acids have been essential for this advance. While at slower pass, synthetic supramolecular chiral glycosystems are also expanding our understanding about helical development and biofunction in living systems. Besides this advance, we are still long way from re-creating and controlling chirality transfer and amplification in complex physiological environment that is abundant of chiral components and out of equilibrium events. Currently, we are limited to perturbing some of these processes by exogenous supplementation of synthetic peptide and glycan amphiphiles or pre-assembled left- and right-handed helices generated from these building blocks. Thus, in spite of the potential of these systems in the development of biofunctional materials, devices and therapies, they are still underexploited in these fields.

Conflicts of interest

There are no conflicts to declare.

Data availability

No primary research results, software or code have been included and no new data were generated or analysed as part of this review.

Acknowledgements

The authors acknowledge the financial support from the European Commission (grants M-ERA-NET3/0007/2021 RePark; and

Open Access Article. Published on 13 August 2025. Downloaded on 1/7/2026 10:35:48 PM. This article is licensed under a Creative Commons Attribution 3.0 Unported Licence.

HORIZON-EIC-2022-PATHFINDEROPEN-01-101099063 Aptadegrad) and the Portuguese Foundation for Science and Technology (FCT) under grants PD/BD/135256/2017 and COVID/BD/152018/2021.

References

1 G. Vantomme and J. Crassous, *Chirality*, 2021, **33**, 597–601.
2 J. Weyer, *Angew. Chem., Int. Ed. Engl.*, 1974, **13**, 591–598.
3 R. B. Grossman, *J. Chem. Educ.*, 1989, **66**, 30–33.
4 L. D. Aubrey, L. Lutter, K. Fennell, T. J. Purton, N. Ward, L. C. Serpell and W.-F. Xue, *bioRxiv*, 2023, preprint, DOI: 10.1101/2023.07.14.549001.
5 D. G. Blackmond, *Cold Spring Harbor Perspect. Biol.*, 2010, **2**, a002147.
6 M. Wang, P. Zhou, J. Wang, Y. Zhao, H. Ma, J. R. Lu and H. Xu, *J. Am. Chem. Soc.*, 2017, **139**, 4185–4194.
7 A. M. Garcia, D. Iglesias, E. Parisi, K. E. Styan, L. J. Waddington, C. Deganutti, R. De Zorzi, M. Grassi, M. Melchionna, A. V. Vargiu and S. Marchesan, *Chem*, 2018, **4**, 1862–1876.
8 H. Wadai, K. Yamaguchi, S. Takahashi, T. Kanno, T. Kawai, H. Naiki and Y. Goto, *Biochemistry*, 2005, **44**, 157–164.
9 A. Brito, S. Kassem, R. L. Reis, R. V. Ulijn, R. A. Pires and I. Pashkuleva, *Chem*, 2021, **7**, 2943–2964.
10 M. Delbianco, P. Bharate, S. Varela-Aramburu and P. H. Seeberger, *Chem. Rev.*, 2016, **116**, 1693–1752.
11 S. Gim, G. Fittolani, Y. Nishiyama, P. H. Seeberger, Y. Ogawa and M. Delbianco, *Angew. Chem., Int. Ed.*, 2020, **59**, 22577–22583.
12 L. Schefer, J. Adamcik, M. Diener and R. Mezzenga, *Nanoscale*, 2015, **7**, 16182–16188.
13 G. Fittolani, P. H. Seeberger and M. Delbianco, *Pept. Sci.*, 2020, **112**, e24124.
14 H. B. Mayes, L. J. Broadbelt and G. T. Beckham, *J. Am. Chem. Soc.*, 2014, **136**, 1008–1022.
15 M. H. Liu, L. Zhang and T. Y. Wang, *Chem. Rev.*, 2015, **115**, 7304–7397.
16 E. Yashima, N. Ousaka, D. Taura, K. Shimomura, T. Ikai and K. Maeda, *Chem. Rev.*, 2016, **116**, 13752–13990.
17 S. Huang, H. Yu and Q. Li, *Adv. Sci.*, 2021, **8**, 2002132.
18 T. F. A. De Greef, M. M. J. Smulders, M. Wolffs, A. P. H. J. Schenning, R. P. Sijbesma and E. W. Meijer, *Chem. Rev.*, 2009, **109**, 5687–5754.
19 S. A. Deshmukh, L. A. Solomon, G. Kamath, H. C. Fry and S. K. R. S. Sankaranarayanan, *Nat. Commun.*, 2016, **7**, 12367.
20 E. Krieg, M. M. C. Bastings, P. Besenius and B. Rybtchinski, *Chem. Rev.*, 2016, **116**, 2414–2477.
21 P. K. Hashim, J. Bergueiro, E. W. Meijer and T. Aida, *Prog. Polym. Sci.*, 2020, **105**, 101250.
22 N. S. S. Nizar, M. Sujith, K. Swathi, C. Sissa, A. Painelli and K. G. Thomas, *Chem. Soc. Rev.*, 2021, **50**, 11208–11226.
23 J. V. Selinger, M. S. Spector and J. M. Schnur, *J. Phys. Chem. B*, 2001, **105**, 7157–7169.
24 A. Aggeli, I. A. Nyrkova, M. Bell, R. Harding, L. Carrick, T. C. B. McLeish, A. N. Semenov and N. Boden, *Proc. Natl. Acad. Sci. U. S. A.*, 2001, **98**, 11857–11862.
25 E. T. Pashuck and S. I. Stupp, *J. Am. Chem. Soc.*, 2010, **132**, 8819–8821.
26 J. H. Fuhrhop, P. Schnieder, E. Boekema and W. Helfrich, *J. Am. Chem. Soc.*, 1988, **110**, 2861–2867.
27 M. Quack, G. Seyfang and G. Wichmann, *Chem. Sci.*, 2022, **13**, 10598–10643.
28 Y. Sang and M. Liu, *Chem. Sci.*, 2022, **13**, 633–656.
29 D. H. Lee, J. R. Granja, J. A. Martinez, K. Severin and M. R. Ghadiri, *Nature*, 1996, **382**, 525–528.
30 J. Nanda, B. Rubinov, D. Ivnitski, R. Mukherjee, E. Shtelman, Y. Motro, Y. Miller, N. Wagner, R. Cohen-Luria and G. Ashkenasy, *Nat. Commun.*, 2017, **8**, 434.
31 S. Maity, J. Ottelé, G. M. Santiago, P. W. J. M. Frederix, P. Kroon, O. Markovitch, M. C. A. Stuart, S. J. Marrink, S. Otto and W. H. Roos, *J. Am. Chem. Soc.*, 2020, **142**, 13709–13717.
32 H. V. Berlepsch, K. Ludwig, B. Schade, R. Haag and C. Böttcher, *Adv. Colloid Interface Sci.*, 2014, **208**, 279–292.
33 L. Yang, X. Dou, C. Ding and C. Feng, *J. Phys. Chem. Lett.*, 2021, **12**, 1155–1161.
34 M. M. Green, M. P. Reidy, R. J. Johnson, G. Darling, D. J. Oleary and G. Willson, *J. Am. Chem. Soc.*, 1989, **111**, 6452–6454.
35 S. K. Jha, K. S. Cheon, M. M. Green and J. V. Selinger, *J. Am. Chem. Soc.*, 1999, **121**, 1665–1673.
36 M. M. Green, B. A. Garetz, B. Munoz, H. P. Chang, S. Hoke and R. G. Cooks, *J. Am. Chem. Soc.*, 1995, **117**, 4181–4182.
37 A. R. A. Palmans and E. W. Meijer, *Angew. Chem., Int. Ed.*, 2007, **46**, 8948–8968.
38 M. Pandeeswar, M. B. Avinash and T. Govindaraju, *Chem. – Eur. J.*, 2012, **18**, 4818–4822.
39 J. Liang, A. Hao, P. Xing and Y. Zhao, *ACS Nano*, 2021, **15**, 5322–5332.
40 T. Y. Yuan, Z. M. Sun, A. U. Mu, M. X. Zeng, A. J. D. Kalin, Z. Cheng, M. A. Olson and L. Fang, *Chem. – Eur. J.*, 2018, **24**, 16553–16557.
41 N. Ousaka, M. J. Maclachlan and S. Akine, *Nat. Commun.*, 2023, **14**, 6834.
42 A. R. A. Palmans, E. W. Meijer and S. E. Denmark, *J. Polym. Sci.*, 2021, **59**, 1171–1174.
43 L. Pauling and R. B. Corey, *Proc. Natl. Acad. Sci. U. S. A.*, 1953, **39**, 253–256.
44 J. H. Fuhrhop, M. Krull and G. Buldt, *Angew. Chem., Int. Ed. Engl.*, 1987, **26**, 699–700.
45 R. J. Swanekamp, J. T. M. DiMaio, C. J. Bowerman and B. L. Nilsson, *J. Am. Chem. Soc.*, 2012, **134**, 5556–5559.
46 Z. Guo, Y. S. Song, Y. J. Wang, T. Y. Tan, Y. W. Ji, G. X. Zhang, J. Hu and Y. Zhang, *Front. Mol. Biosci.*, 2021, **8**, 700964.
47 J. H. Fuhrhop and C. Boettcher, *J. Am. Chem. Soc.*, 1990, **112**, 1768–1776.
48 A. X. Wu and L. Isaacs, *J. Am. Chem. Soc.*, 2003, **125**, 4831–4835.
49 M. H. Sangji, S. R. Lee, H. Sai, S. Weigand, L. C. Palmer and S. I. Stupp, *ACS Nano*, 2024, **18**, 15878–15887.
50 A. Brito, D. Dave, A. Lampel, V. I. B. Castro, D. Kroiss, R. L. Reis, T. Tuttle, R. V. Ulijn, R. A. Pires and I. Pashkuleva, *J. Am. Chem. Soc.*, 2021, **143**, 19703–19710.

Open Access Article. Published on 13 August 2025. Downloaded on 1/7/2026 10:35:48 PM. This article is licensed under a Creative Commons Attribution 3.0 Unported Licence.

51 S. Gim, G. Fittolani, Y. Yu, Y. Zhu, P. H. Seeberger, Y. Ogawa and M. Delbianco, *Chemistry*, 2021, **27**, 13139–13143.
52 V. I. B. Castro, Y. T. Gao, A. Brito, J. Chen, R. L. Reis, I. Pashkuleva and R. A. Pires, *J. Mater. Chem. B*, 2024, **12**, 6996–7000.
53 N. Yadav, S. Djalali, A. Poveda, M. G. Ricardo, P. H. Seeberger, J. Jiménez-Barbero and M. Delbianco, *J. Am. Chem. Soc.*, 2024, **146**, 6369–6376.
54 J. H. Fuhrhop, P. Schnieder, J. Rosenberg and E. Boekema, *J. Am. Chem. Soc.*, 1987, **109**, 3387–3390.
55 N. Nakashima, S. Asakuma and T. Kunitake, *J. Am. Chem. Soc.*, 1985, **107**, 509–510.
56 K. Qi, H. Qi, M. Wang, X. Ma, Y. Wang, Q. Yao, W. Liu, Y. Zhao, J. Wang, Y. Wang, W. Qi, J. Zhang, J. R. Lu and H. Xu, *Nat. Commun.*, 2024, **15**, 6186.
57 Q. G. Xing, J. X. Zhang, Y. Y. Xie, Y. F. Wang, W. Qi, H. J. Rao, R. X. Su and Z. M. He, *ACS Nano*, 2018, **12**, 12305–12314.
58 S. J. Klawa, M. C. L. Lee, K. D. Riker, T. Y. Jian, Q. Z. Wang, Y. Gao, M. L. Daly, S. Bhonge, W. S. Childers, T. O. Omosun, A. K. Mehta, D. G. Lynn and R. Freeman, *Nat. Commun.*, 2024, **15**, 788.
59 B. Pfannemuller and W. Welte, *Chem. Phys. Lipids*, 1985, **37**, 227–240.
60 V. Zabel, A. Mullerfahrnow, R. Hilgenfeld, W. Saenger, B. Pfannemuller, V. Enkelmann and W. Welte, *Chem. Phys. Lipids*, 1986, **39**, 313–327.
61 Y. T. Fu, B. Z. Li, Z. B. Huang, Y. Li and Y. G. Yang, *Langmuir*, 2013, **29**, 6013–6017.
62 G. Zhang, L. Zhang, H. Rao, Y. Wang, Q. Li, W. Qi, X. Yang, R. Su and Z. He, *J. Colloid Interface Sci.*, 2020, **577**, 388–396.
63 M. G. Qin, Y. Q. Zhang, C. Xing, L. Yang, C. L. Zhao, X. Q. Dou and C. L. Feng, *Chem. – Eur. J.*, 2021, **27**, 3119–3129.
64 C. Nacar, *Protein J.*, 2022, **41**, 551–562.
65 A. Chakrabartty, A. J. Doig and R. L. Baldwin, *Proc. Natl. Acad. Sci. U. S. A.*, 1993, **90**, 11332–11336.
66 R. B. Best, D. de Sancho and J. Mittal, *Biophys. J.*, 2012, **102**, 1462–1467.
67 S. Svenson, J. Koning and J. H. Fuhrhop, *J. Phys. Chem.*, 1994, **98**, 1022–1028.
68 C. Boettcher, H. Stark and M. vanHeel, *Ultramicroscopy*, 1996, **62**, 133–139.
69 K. Bag, K. Naresh and N. Jayaraman, *Mater. Today Chem.*, 2022, **26**, 101026.
70 K. R. Wang, H. W. An, L. Wu, J. C. Zhang and X. L. Li, *Chem. Commun.*, 2012, **48**, 5644–5646.
71 G. Fittolani, T. Tyrikos-Ergas, A. Poveda, Y. Yu, N. Yadav, P. H. Seeberger, J. Jiménez-Barbero and M. Delbianco, *Nat. Chem.*, 2023, **15**, 1461–1469.
72 S. Djalali, N. Yadav and M. Delbianco, *Nat. Rev. Mater.*, 2024, **9**, 190–201.
73 A. Chakrabartty, T. Kortemme and R. L. Baldwin, *Protein Sci.*, 1994, **3**, 843–852.
74 P. Morales and M. A. Jiménez, *Arch. Biochem. Biophys.*, 2019, **661**, 149–167.
75 P. Kumar, N. G. Paterson, J. Clayden and D. N. Woolfson, *Nature*, 2022, **607**, 387–392.
76 A. A. Adzhubei, M. J. E. Sternberg and A. A. Makarov, *J. Mol. Biol.*, 2013, **425**, 2100–2132.
77 Q. Song, Z. Cheng, M. Kariuki, S. C. L. Hall, S. K. Hill, J. Y. Rho and S. Perrier, *Chem. Rev.*, 2021, **121**, 13936–13995.
78 J. L. Beesley and D. N. Woolfson, *Curr. Opin. Biotechnol.*, 2019, **58**, 175–182.
79 T. O. Yeates, *Annu. Rev. Biophys.*, 2017, **46**, 23–42.
80 X. S. Yan, P. M. Weng, D. Shi and Y. B. Jiang, *Chem. Commun.*, 2021, **57**, 12562–12574.
81 M. Amorin, L. Castedo and J. R. Granja, *Chem. – Eur. J.*, 2008, **14**, 2100–2111.
82 T. Kurita and K. Numata, *Phys. Chem. Chem. Phys.*, 2024, **26**, 28776–28792.
83 C. Dondi, J. Garcia-Ruiz, E. Hasan, S. Rey, J. E. Noble, A. Hoose, A. Briones, I. E. Kepiro, N. Faruqui, P. Aggarwal, P. Ghai, M. Shaw, A. T. Fry, A. Maxwell, B. W. Hoogenboom, C. D. Lorenz and M. G. Ryadnov, *Nat. Commun.*, 2025, **16**, 4535.
84 D. N. Woolfson, *J. Mol. Biol.*, 2021, **433**, 167160.
85 J. Walshaw, J. M. Shipway and D. N. Woolfson, *Biochem. Soc. Symp.*, 2001, **68**, 111–123.
86 I. Drobnak, H. Gradisar, A. Ljubetic, E. Merljak and R. Jerala, *J. Am. Chem. Soc.*, 2017, **139**, 8229–8236.
87 T. Plaper, E. Rihtar, T. Zeleznik Ramuta, V. Forstneric, V. Jazbec, F. Ivanovski, M. Bencina and R. Jerala, *Cell Chem. Biol.*, 2024, **31**, 1460–1472.
88 A. R. Perez, A. Adewole, D. Sihwa, M. E. Colvin and A. D. Merg, *J. Am. Chem. Soc.*, 2024, **146**, 30252–30261.
89 L. T. Yu, M. A. B. Kreutzberger, T. H. Bui, M. C. Hancu, A. C. Farsheed, E. H. Egelman and J. D. Hartgerink, *Nat. Commun.*, 2024, **15**, 10385.
90 L. E. R. O'Leary, J. A. Fallas, E. L. Bakota, M. K. Kang and J. D. Hartgerink, *Nat. Chem.*, 2011, **3**, 821–828.
91 D. N. Woolfson, *Adv. Protein Chem.*, 2005, **70**, 79–112.
92 F. Lapenta, J. Aupic, Z. Strmsek and R. Jerala, *Chem. Soc. Rev.*, 2018, **47**, 3530–3542.
93 D. Britton, J. W. Sun, P. D. Renfrew and J. K. Montclare, *Annu. Rev. Chem. Biomol. Eng.*, 2024, **15**, 25–50.
94 I. Helmers, G. Ghosh, R. Q. Albuquerque and G. Fernández, *Angew. Chem., Int. Ed.*, 2021, **60**, 4368–4376.
95 A. Pross and R. Pascal, *Beilstein J. Org. Chem.*, 2017, **13**, 665–674.
96 M. Kollmer, W. Close, L. Funk, J. Rasmussen, A. Bsoul, A. Schierhorn, M. Schmidt, C. J. Sigurdson, M. Jucker and M. Fändrich, *Nat. Commun.*, 2019, **10**, 4760.
97 S. Y. Li, T. Chen, Q. Chen, D. Wang and G. S. Zhu, *Chem. Sci.*, 2023, **14**, 2646–2651.
98 Y. F. Wang, W. Qi, R. L. Huang, X. J. Yang, M. F. Wang, R. X. Su and Z. M. He, *J. Am. Chem. Soc.*, 2015, **137**, 7869–7880.
99 P. Qin, Z. Wu, P. Li, D. Niu, M. Liu and M. Yin, *ACS Appl. Mater. Interfaces*, 2021, **13**, 18047–18055.
100 L. D. Aubrey, B. J. F. Blakeman, L. Lutter, C. J. Serpell, M. F. Tuite, L. C. Serpell and W. F. Xue, *Commun. Chem.*, 2020, **3**, 125.

 This journal is © The Royal Society of Chemistry 2025

Open Access Article. Published on 13 August 2025. Downloaded on 1/7/2026 10:35:48 PM. This article is licensed under a Creative Commons Attribution 3.0 Unported Licence.

101 X. Periole, T. Huber, A. Bonito-Oliva, K. C. Aberg, P. C. A. van der Wel, T. P. Sakmar and S. J. Marrink, *J. Phys. Chem. B*, 2018, **122**, 1081–1091.
102 L. R. Volpatti, M. Vendruscolo, C. M. Dobson and T. P. J. Knowles, *ACS Nano*, 2013, **7**, 10443–10448.
103 S. Xue, P. Xing, J. Zhang, Y. Zeng and Y. Zhao, *Chemistry*, 2019, **25**, 7426–7437.
104 Y. Li, B. Z. Li, Y. T. Fu, S. W. Lin and Y. G. Yang, *Langmuir*, 2013, **29**, 9721–9726.
105 M. Kataria, Y. Kim, H. D. Chau, N. Y. Kwon, Y. Hong, T. Kim, J. Ko, M. K. Son, J. Bang, S. Park, H. I. Kim, K. Lee and D. H. Choi, *J. Mater. Chem. C*, 2022, **10**, 10679–10685.
106 N. Gao, Z. Du, Y. Guan, K. Dong, J. Ren and X. Qu, *J. Am. Chem. Soc.*, 2019, **141**, 6915–6921.
107 L. A. Schneider, A. Korber, S. Grabbe and J. Dissemond, *Arch. Dermatol. Res.*, 2007, **298**, 413–420.
108 M. Hatip Koc, G. Cinar Ciftci, S. Baday, V. Castelletto, I. W. Hamley and M. O. Guler, *Langmuir*, 2017, **33**, 7947–7956.
109 A. Kousar, J. Liu, N. Mehwish, F. Wang, A. Y. Dang-i and C. Feng, *Mater. Today Chem.*, 2019, **11**, 217–224.
110 S. Wang, M. C. Forster, K. Xue, F. Ehlers, B. Pang, L. B. Andreas, P. Vana and K. Zhang, *Angew. Chem., Int. Ed.*, 2021, **60**, 9712–9718.
111 S. Debnath, S. Roy, Y. M. Abul-Haija, P. Frederix, S. Ramalhete, A. Hirst, N. Javid, N. Hunt, S. Kelly, J. Angulo, Y. Khimyak and R. Ulijn, *Chemistry*, 2019, **25**, 7881–7887.
112 J. X. Cui, A. H. Liu, Y. Guan, J. Zheng, Z. H. Shen and X. H. Wan, *Langmuir*, 2010, **26**, 3615–3622.
113 L. Gao, C. Xing, X. Dou, Y. Zou, C. Zhao and C. Feng, *Angew. Chem., Int. Ed.*, 2022, **61**, e202211812.
114 M. Go, H. Choi, K. Y. Kim, C. J. Moon, Y. Choi, H. Miyake, S. S. Lee, S. H. Jung, M. Y. Choi and J. H. Jung, *Org. Chem. Front.*, 2019, **6**, 1100–1108.
115 J. George, S. Kar, E. S. Anupriya, S. M. Somasundaran, A. D. Das, C. Sissa, A. Painelli and K. G. Thomas, *ACS Nano*, 2019, **13**, 4392–4401.
116 M. Ok, K. Y. Kim, H. Choi, S. Kim, S. S. Lee, J. Cho, S. H. Jung and J. H. Jung, *Chem. Sci.*, 2022, **13**, 3109–3117.
117 J. Adamcik and R. Mezzenga, *Soft Matter*, 2011, **7**, 5437–5443.
118 X. Wang and C. Feng, *Wiley Interdiscip. Rev.: Nanomed. Nanobiotechnol.*, 2023, **15**, e1847.
119 Y. Wang, X. Zhang, K. Wan, N. Zhou, G. Wei and Z. Su, *J. Nanobiotechnol.*, 2021, **19**, 253.
120 Z. Du, B. Fan, Q. Dai, L. Wang, J. Guo, Z. Ye, N. Cui, J. Chen, K. Tan, R. Li and W. Tang, *Giant*, 2022, **9**, 100082.
121 C. M. E. Kriebisch, O. Bantysh, L. B. Pellejero, A. Belluati, E. Bertosin, K. Dai, M. de Roy, H. L. Fu, N. Galvanetto, J. M. Gibbs, S. S. Gomez, G. Granatelli, A. Griffo, M. Guix, C. O. Gurdap, J. Harth-Kitzerow, I. S. Haugerud, G. Häfner, P. Jaiswal, S. Javed, A. Karimi, S. Kato, B. A. K. Kriebisch, S. Laha, P. W. Lee, W. P. Lipinski, T. Matreux, T. C. T. Michaels, E. Poppleton, A. Ruf, A. D. Slootbeek, I. B. A. Smokers, H. Soria-Carrera, A. Sorrenti, M. Stasi, A. Stevenson, A. Thatte, M. Tran, M. H. I. van Haren, H. D. Vuijk, S. F. J. Wickham, P. Zambrano, K. P. Adamala, K. Alim, E. S. Andersen, C. Bonfio, D. Braun, E. Frey, U. Gerland, W. T. S. Huck, F. Jülicher, N. Laohakunakorn, L. Mahadavan, S. Otto, J. Saenz, P. Schwille, K. Göpfrich, C. A. Weber and J. Boekhoven, *Chem*, 2025, **11**, 102399.
122 P. Adamski, M. Eleveld, A. Sood, A. Kun, A. Szilágyi, T. Czárán, E. Szathmáry and S. Otto, *Nat. Rev. Chem.*, 2020, **4**, 386–403.
123 J. M. A. Carnall, C. A. Waudby, A. M. Belenguer, M. C. A. Stuart, J. J. P. Peyralans and S. Otto, *Science*, 2010, **327**, 1502–1506.
124 M. Colomb-Delsuc, E. Mattia, J. W. Sadownik and S. Otto, *Nat. Commun.*, 2015, **6**, 7427.
125 S. Yang, Y. Geiger, M. Geerts, M. J. Eleveld, A. Kiani and S. Otto, *J. Am. Chem. Soc.*, 2023, **145**, 16889–16898.
126 D. Eisenberg and M. Jucker, *Cell*, 2012, **148**, 1188–1203.
127 A. R. Foley and J. A. Raskatov, *Curr. Opin. Chem. Biol.*, 2021, **64**, 1–9.
128 M. L. Choi and S. Gandhi, *FEBS J.*, 2018, **285**, 3631–3644.
129 A. W. P. Fitzpatrick, G. T. Debelouchina, M. J. Bayro, D. K. Clare, M. A. Caporini, V. S. Bajaj, C. P. Jaroniec, L. C. Wang, V. Ladizhansky, S. A. Müller, C. E. MacPhee, C. A. Waudby, H. R. Mott, A. De Simone, T. P. J. Knowles, H. R. Saibil, M. Vendruscolo, E. V. Orlova, R. G. Griffin and C. M. Dobson, *Proc. Natl. Acad. Sci. U. S. A.*, 2013, **110**, 5468–5473.
130 F. Kametani and M. Hasegawa, *Front. Neurosci.*, 2018, **12**, 25.
131 S. Bera, B. Xue, P. Rehak, G. Jacoby, W. Ji, L. J. W. Shimon, R. Beck, P. Král, Y. Cao and E. Gazit, *ACS Nano*, 2020, **14**, 1694–1706.
132 S. Dutta, T. S. Finn, A. J. Kuhn, B. Abrams and J. A. Raskatov, *ChemBioChem*, 2019, **20**, 1023–1026.
133 S. Dutta, A. R. Foley, C. J. A. Warner, X. Zhang, M. Rolandi, B. Abrams and J. A. Raskatov, *Angew. Chem., Int. Ed.*, 2017, **56**, 11506–11510.
134 K. Hou, J. Zhao, H. Wang, B. Li, K. Li, X. Shi, K. Wan, J. Ai, J. Lv, D. Wang, Q. Huang, H. Wang, Q. Cao, S. Liu and Z. Tang, *Nat. Commun.*, 2020, **11**, 4790.
135 J. Liu, F. Yuan, X. Ma, D. Y. Auphedeous, C. Zhao, C. Liu, C. Shen and C. Feng, *Angew. Chem., Int. Ed.*, 2018, **57**, 6475–6479.
136 Y. Wang, Y. Yang, X. Wang, T. Yoshitomi, N. Kawazoe, Y. Yang and G. Chen, *Biomaterials*, 2021, **271**, 120751.
137 X. Dou, N. Mehwish, C. Zhao, J. Liu, C. Xing and C. Feng, *Acc. Chem. Res.*, 2020, **53**, 852–862.
138 X. Dou, B. Wu, J. Liu, C. Zhao, M. Qin, Z. Wang, H. Schonherr and C. Feng, *ACS Appl. Mater. Interfaces*, 2019, **11**, 38568–38577.
139 N. Sun, X. Dou, Z. Tang, D. Zhang, N. Ni, J. Wang, H. Gao, Y. Ju, X. Dai, C. Zhao, P. Gu, J. Ji and C. Feng, *Bioact. Mater.*, 2021, **6**, 990–997.
140 Y. Wei, S. Jiang, M. Si, X. Zhang, J. Liu, Z. Wang, C. Cao, J. Huang, H. Huang, L. Chen, S. Wang, C. Feng, X. Deng and L. Jiang, *Adv. Mater.*, 2019, **31**, e1900582.

Open Access Article. Published on 13 August 2025. Downloaded on 1/7/2026 10:35:48 PM.
This article is licensed under a Creative Commons Attribution 3.0 Unported Licence.

141 S. Kralj, O. Bellotto, E. Parisi, A. M. Garcia, D. Iglesias, S. Semeraro, C. Deganutti, P. D'Andrea, A. V. Vargiu, S. Geremia, R. De Zorzi and S. Marchesan, *ACS Nano*, 2020, **14**, 16951–16961.
142 K. Sato, W. Ji, Z. Alvarez, L. C. Palmer and S. I. Stupp, *ACS Biomater. Sci. Eng.*, 2019, **5**, 2786–2792.
143 H. Jiang, R. Liu, L. Wang, X. Wang, M. Zhang, S. Lin, Z. Cao, F. Wu, Y. Liu and J. Liu, *Adv. Mater.*, 2023, **35**, e2208157.
144 G. F. Liu, D. Zhang and C. L. Feng, *Angew. Chem., Int. Ed.*, 2014, **53**, 7789–7793.
145 J. F. Shi, X. W. Du, D. Yuan, J. Zhou, N. Zhou, Y. B. Huang and B. Xu, *Biomacromolecules*, 2014, **15**, 3559–3568.
146 Y. Takada, H. Itoh, A. Paudel, S. Panthee, H. Hamamoto, K. Sekimizu and M. Inoue, *Nat. Commun.*, 2020, **11**, 4935.
147 D. T. Bong, T. D. Clark, J. R. Granja and M. R. Ghadiri, *Angew. Chem., Int. Ed.*, 2001, **40**, 988–1011.
148 Z. Ye, X. Zhu, S. Acosta, D. Kumar, T. Sang and C. Aparicio, *Nanoscale*, 2018, **11**, 266–275.
149 Y. Y. Xie, X. T. Qin, J. Zhang, M. Y. Sun, F. P. Wang, M. Huang, S. R. Jia, W. Qi, Y. Wang and C. Zhong, *J. Colloid Interface Sci.*, 2022, **622**, 135–146.
150 S. Baddi, I. A. Dang, T. Huang, C. Xing, S. Lin and C. L. Feng, *Acta Biomater.*, 2022, **141**, 59–69.
151 Q. K. Li, J. Z. Li, W. K. Yu, Z. H. Wang, J. W. Li, X. J. Feng, J. J. Wang and A. S. Shan, *J. Nanobiotechnol.*, 2021, **19**, 183.
152 Y. B. Lim, S. Park, E. Lee, J. H. Ryu, Y. R. Yoon, T. H. Kim and M. Lee, *Chem. – Asian J.*, 2007, **2**, 1363–1369.
153 D. W. Lee, T. Kim, I. S. Park, Z. Huang and M. Lee, *J. Am. Chem. Soc.*, 2012, **134**, 14722–14725.
154 L. M. Chen, X. Zhou, Y. Y. Huang, X. Wang, X. Q. Gao, Y. Cao, W. F. Li and Y. L. Zhou, *Nano Lett.*, 2025, **25**, 1558–1566.
155 Y. Yao, Q. Tang, S. Rosenfeldt, M. Krusmann, M. Karg and K. Zhang, *Small*, 2021, **17**, e2102938.
156 T. Misawa, Y. Kanda and Y. Demizu, *Bioconjugate Chem.*, 2017, **28**, 3029–3035.
157 W. G. Jiang, D. Athanasiadou, S. D. Zhang, R. Demichelis, K. B. Koziara, P. Raiteri, V. Nelea, W. B. Mi, J. A. Ma, J. D. Gale and M. D. McKee, *Nat. Commun.*, 2019 **10**, 2318.
158 S. H. Jung, J. Jeon, H. Kim, J. Jaworski and J. H. Jung, *J. Am. Chem. Soc.*, 2014, **136**, 6446–6452.

 This journal is © The Royal Society of Chemistry 2025